Chain length effect of spiro-ring N-alkylation on photophysical signalling parameters in Fe(III) selective Rhodamine probes

Suryakanta Dehuri,[a,b] Santosh Kumar Mishra[a] and Bamaprasad Bag*[,a,b]

[a] Materials Chemistry Department, CSIR-Institute of Minerals and Materials Technology, Bhubaneswar 751 013, Odisha, India. Email: *bpbag@immt.res.in*

[b] Academy of Scientific and Innovative Research (AcSIR), Ghaziabad- 201002, India.

Electronic Supplementary Information

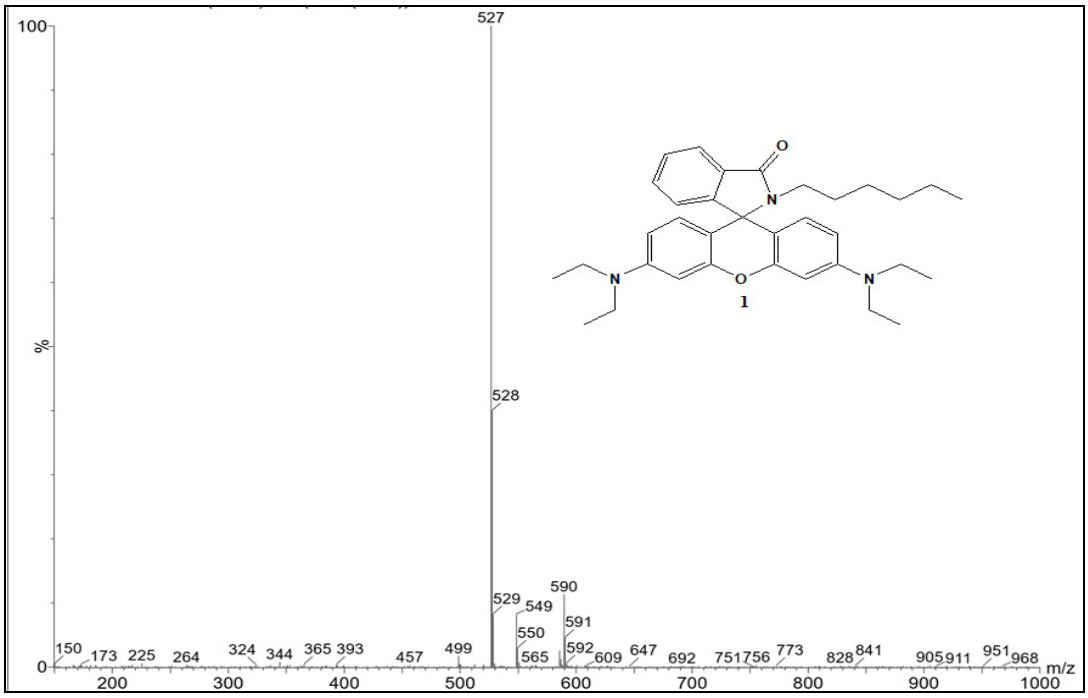

Fig. S1: MS (ESI) spectrum of compound **1**.

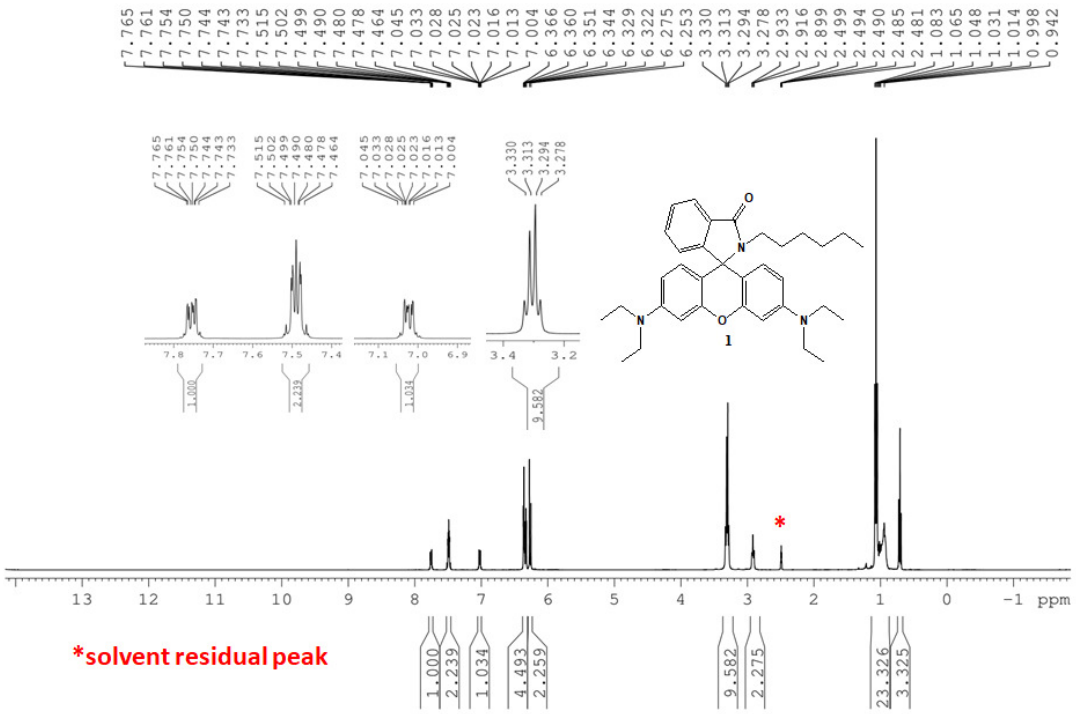

Fig. S2: ^{1}H NMR spectrum of compound **1** (in DMSO-d_6, 400MHz)

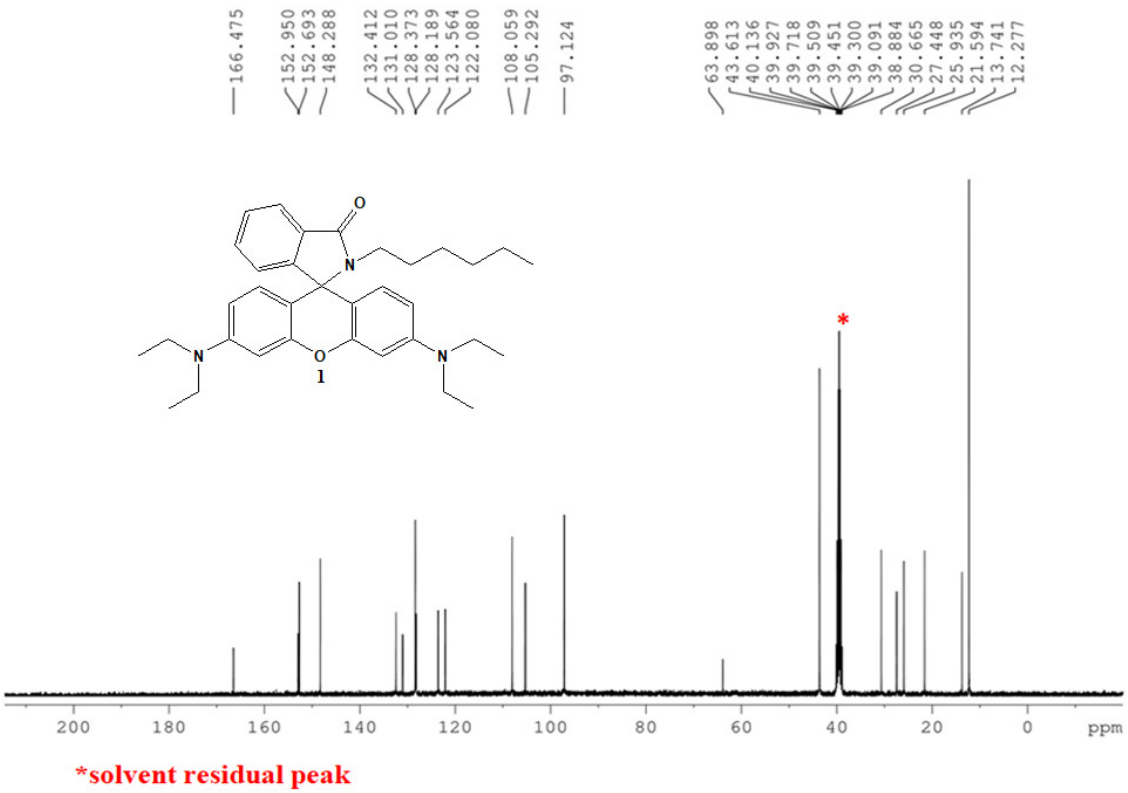

Fig. S3: ^{13}C NMR spectrum of compound **1** (in DMSO-d_6).

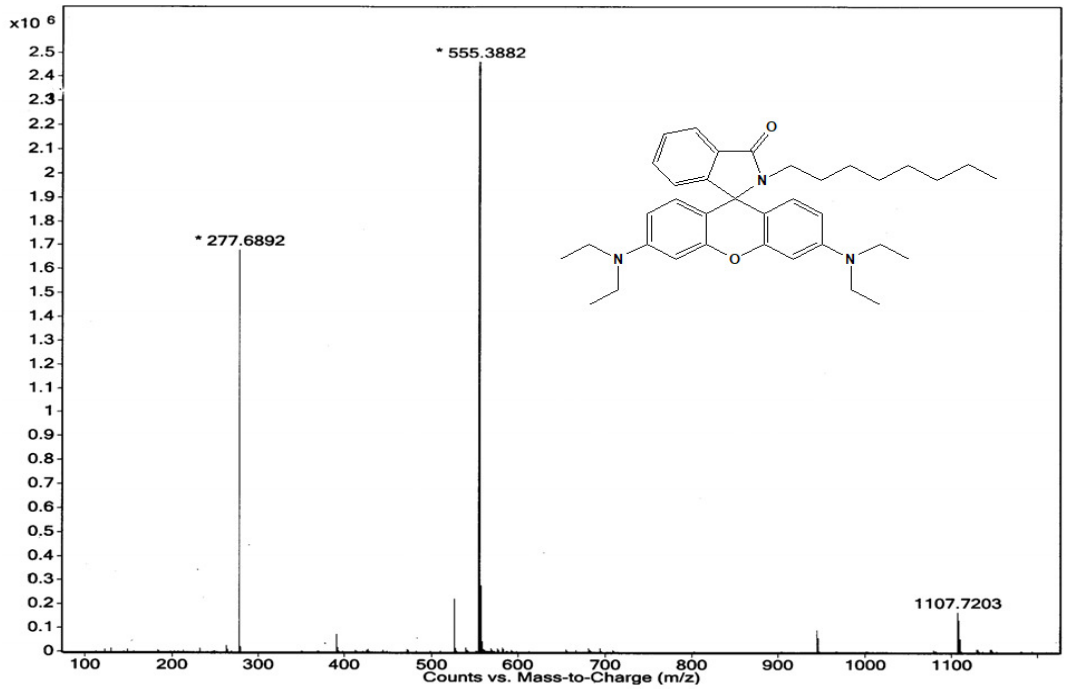

Fig. S4: MS (ESI) spectrum of compound **2**.

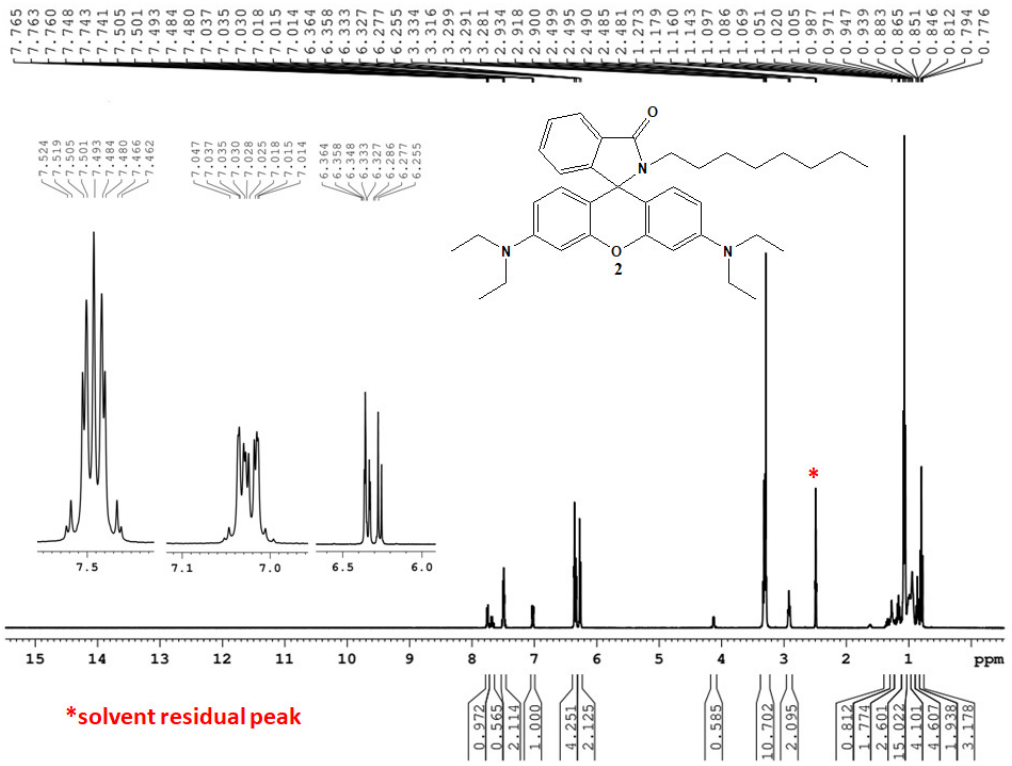

Fig. S5: ^{1}H NMR spectrum of compound **2** (in DMSO-d_6)

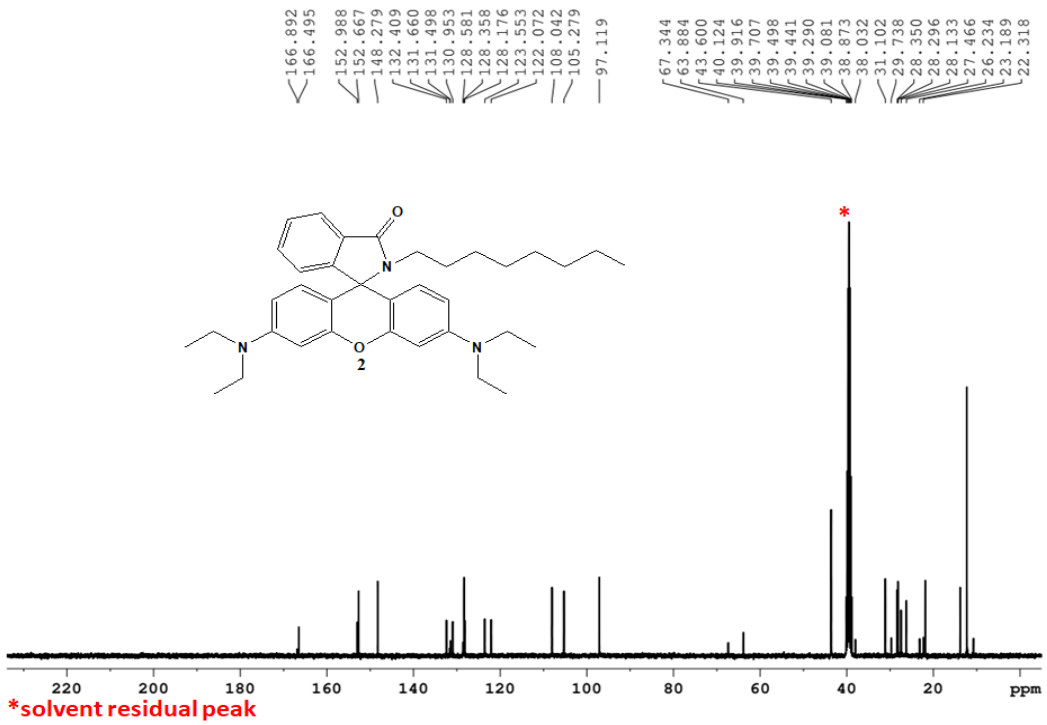

Fig. S6: ^{13}C NMR spectrum of compound **2** (in DMSO-d_6).

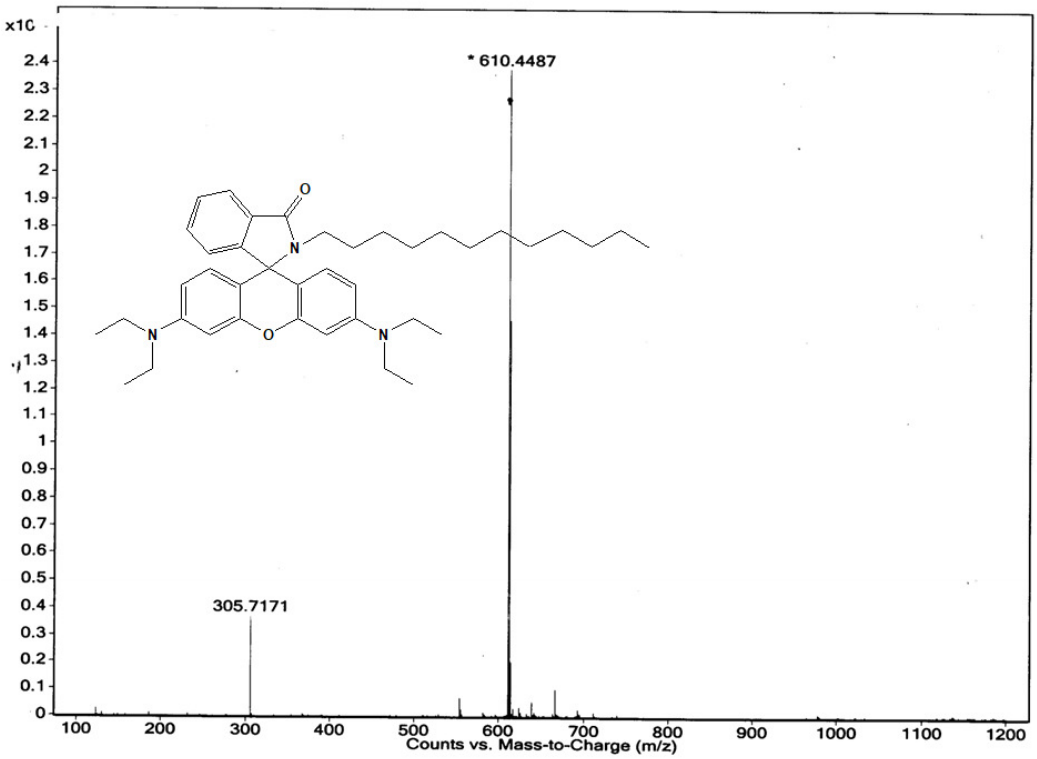

Fig. S7: MS (ESI) spectrum of compound **3**.

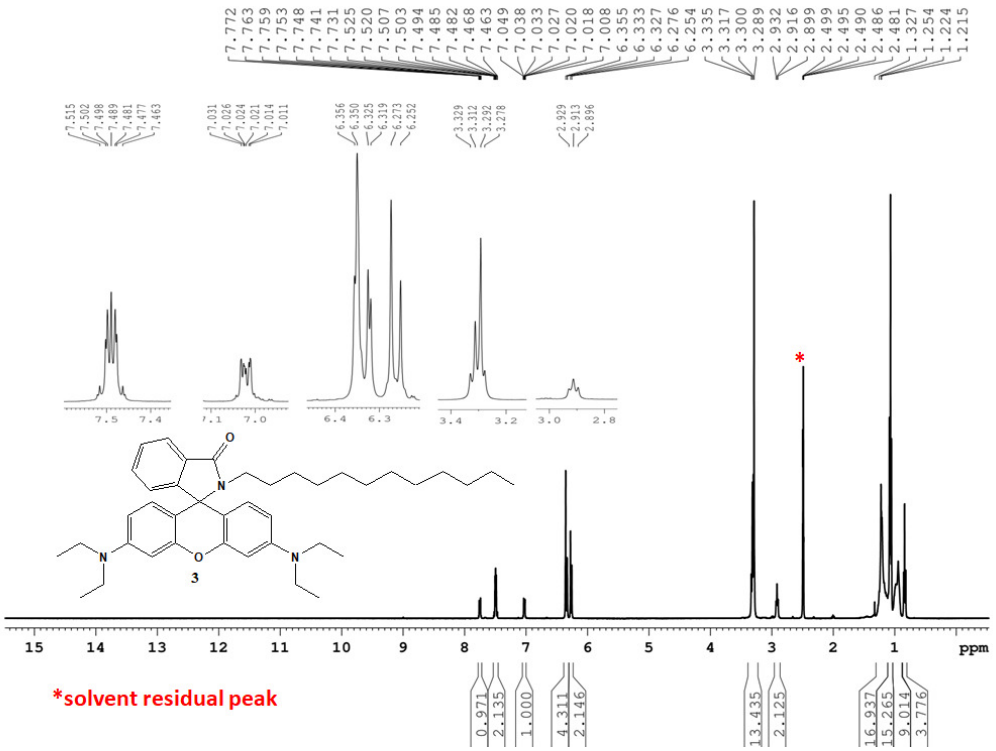

Fig. S8: ^{1}H NMR spectrum of compound **3** (in DMSO-d_6)

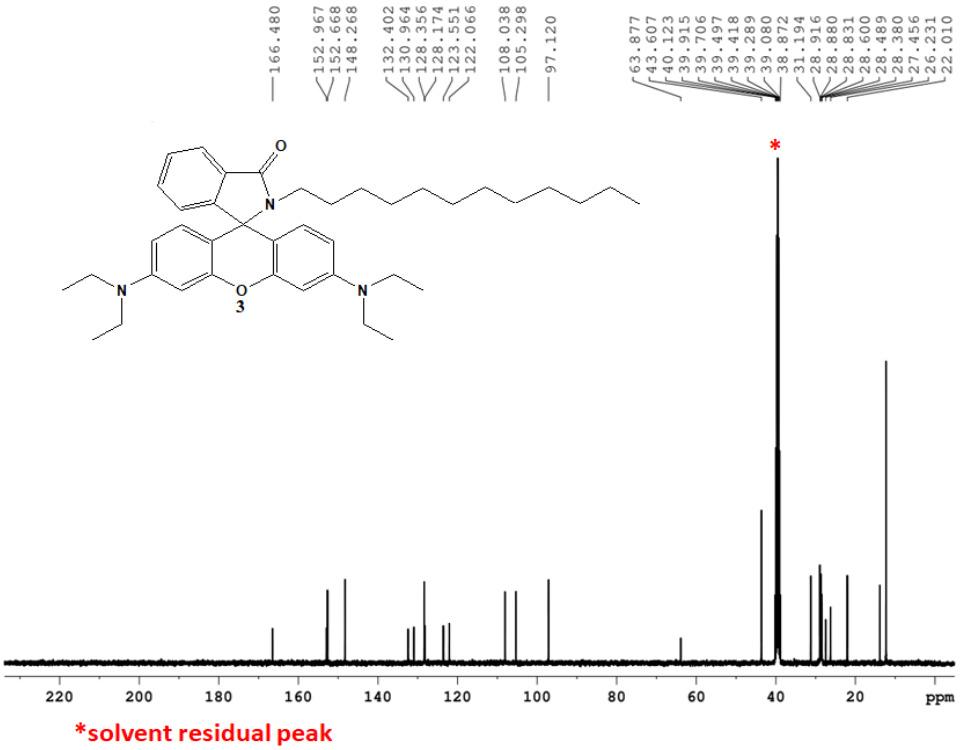

Fig. S9: ^{13}C NMR spectrum of compound **3** (in DMSO-d_6).

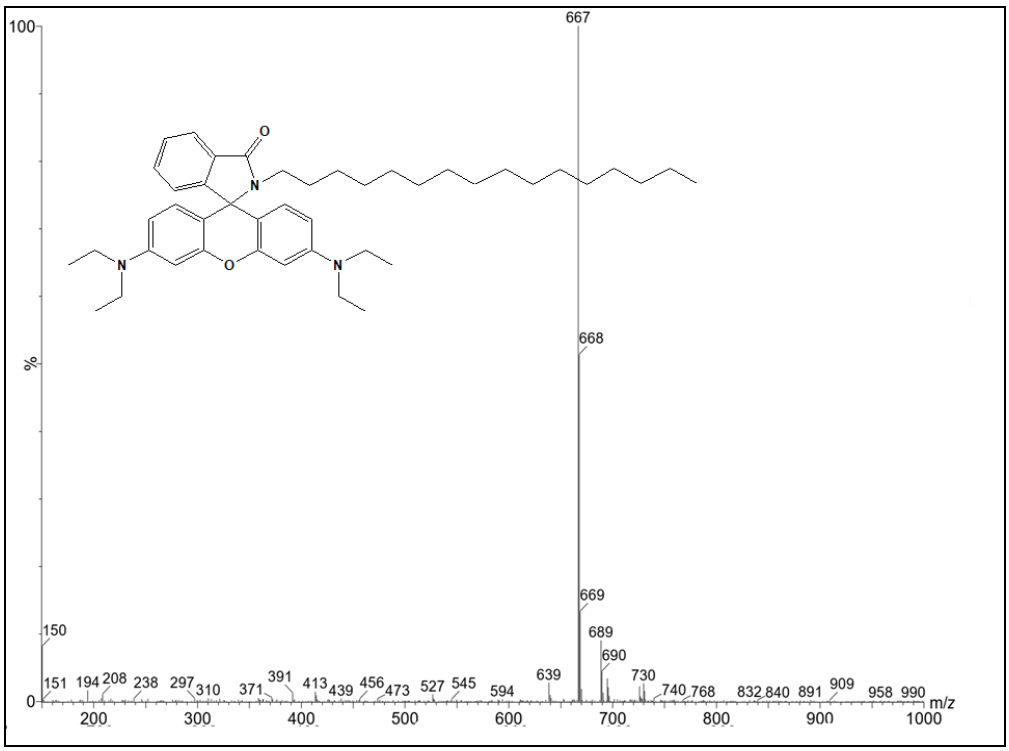

Fig. S10: MS (ESI) spectrum of compound **4**.

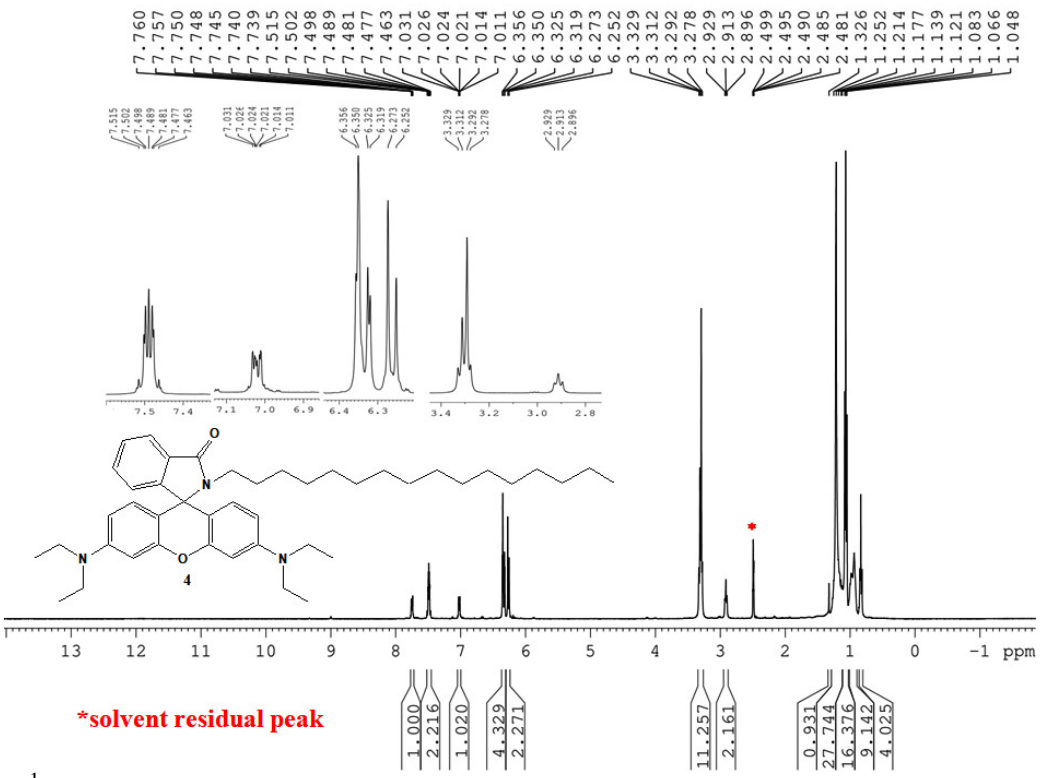

Fig. S11: ^{1}H NMR spectrum of compound **4** (in DMSO-d_6)

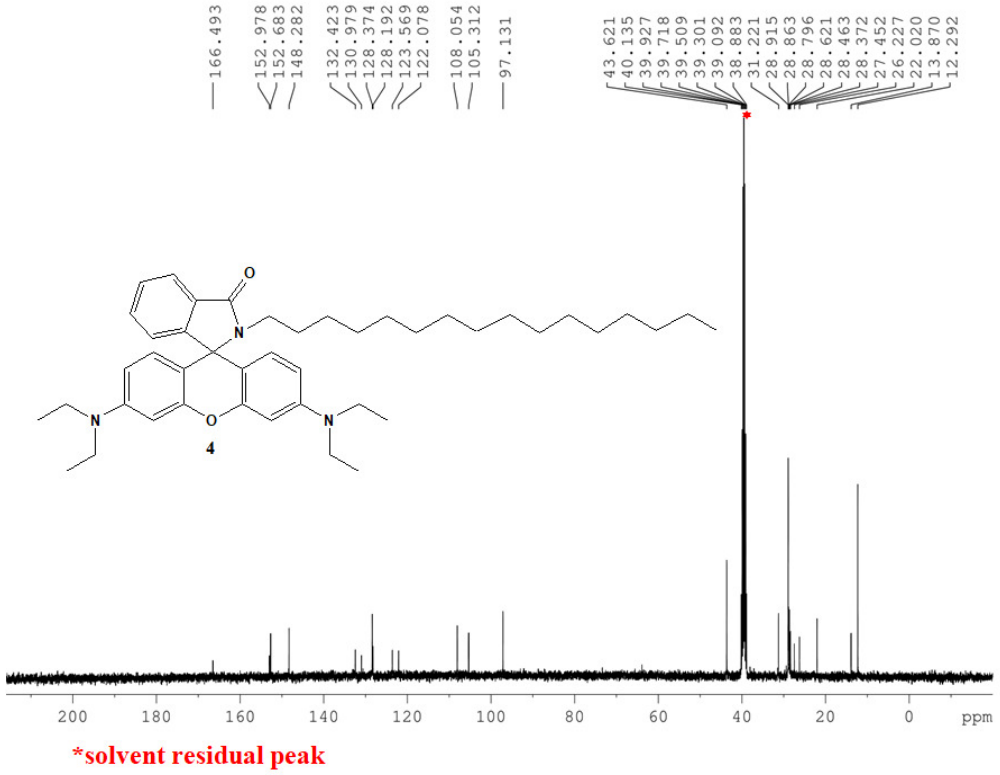

Fig. S12: ^{13}C NMR spectrum of compound **4** (in DMSO-d_6).

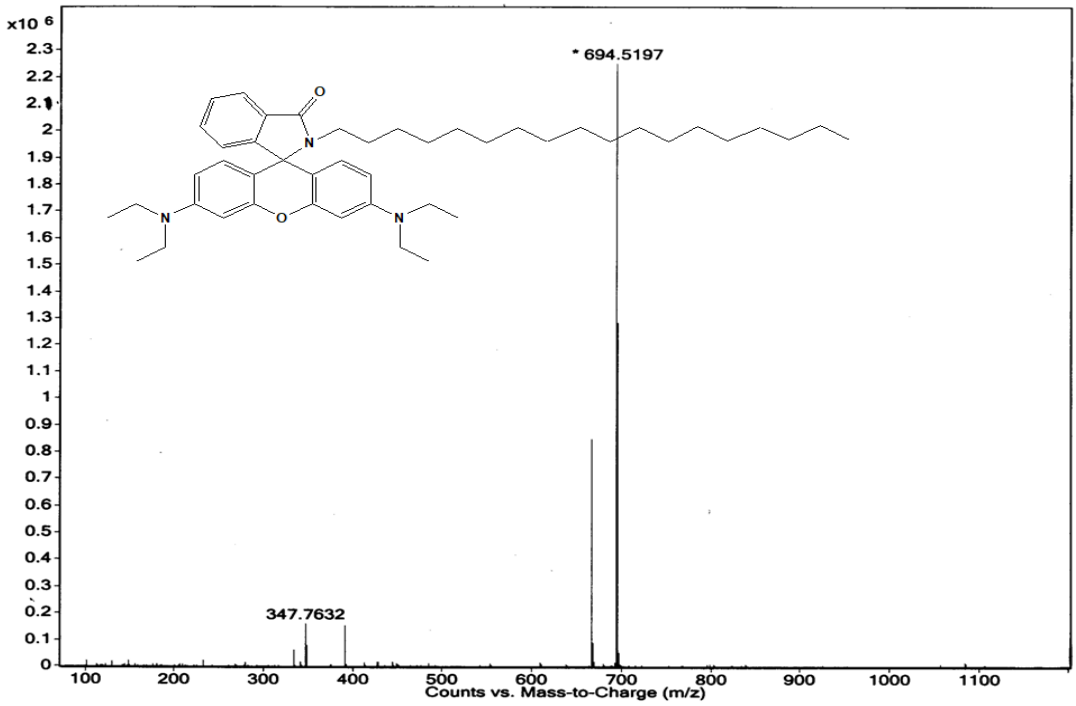

Fig. S13: MS (ESI) spectrum of compound **5**.

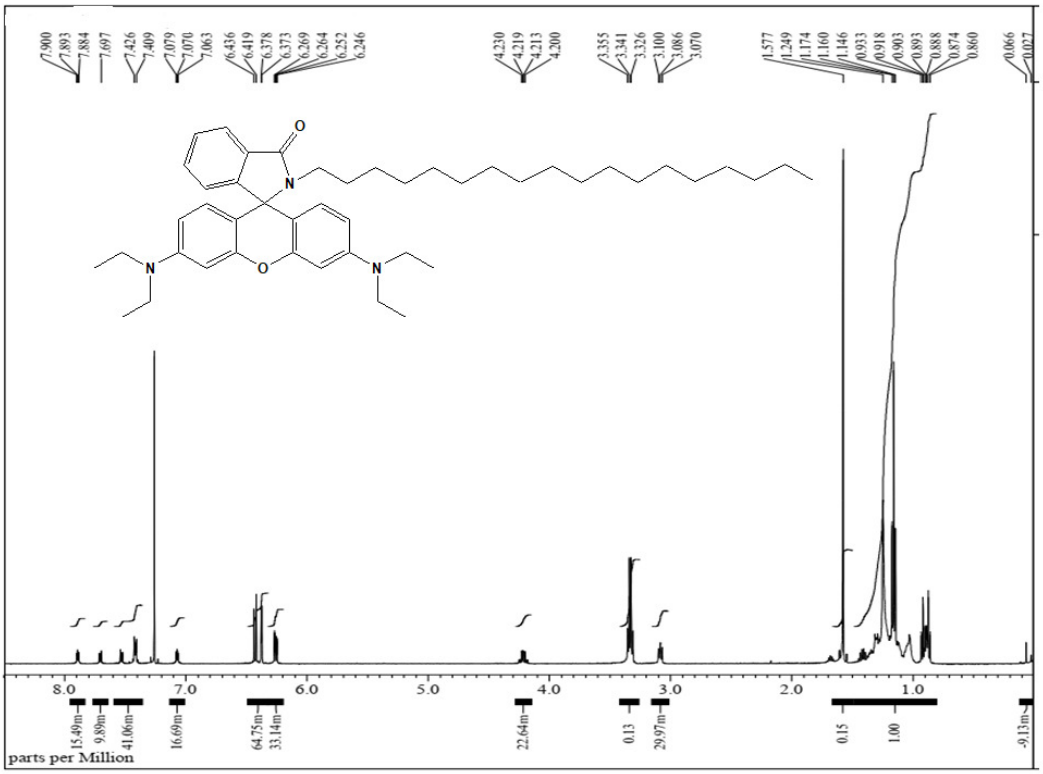

Fig. S14: ^{1}H NMR spectrum of compound **5** (in $CDCl_3$)

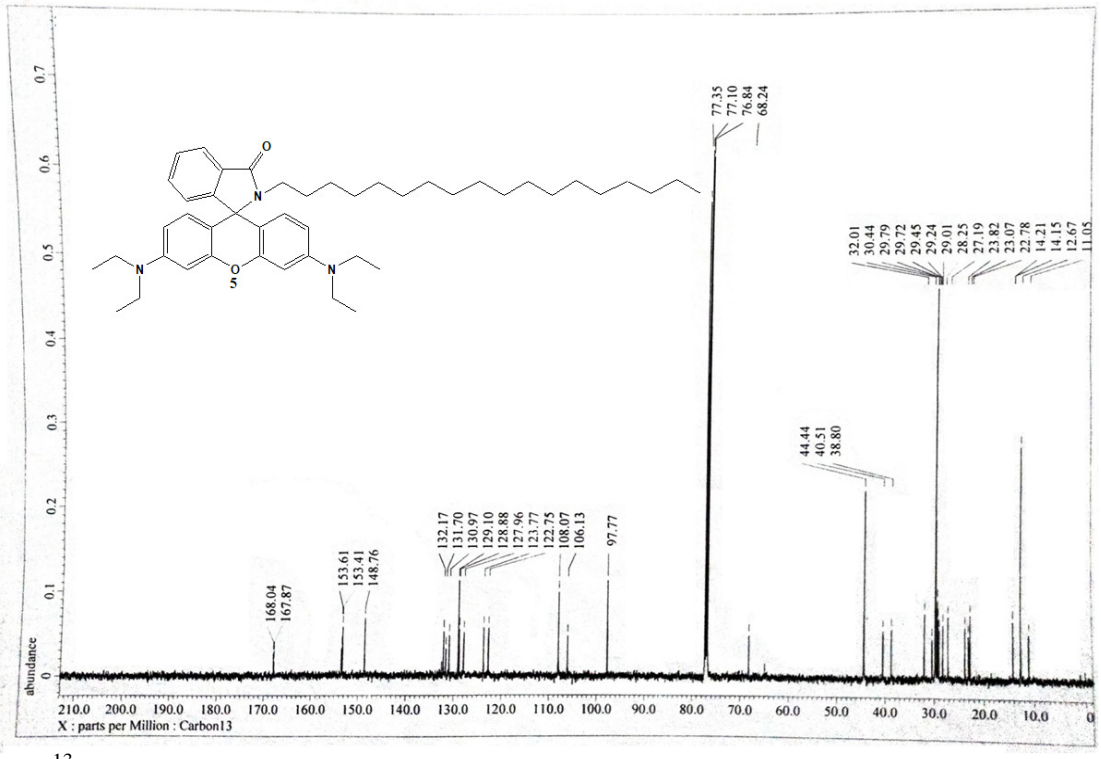

Fig. S15: ^{13}C NMR spectrum of compound **5** (in $CDCl_3$)

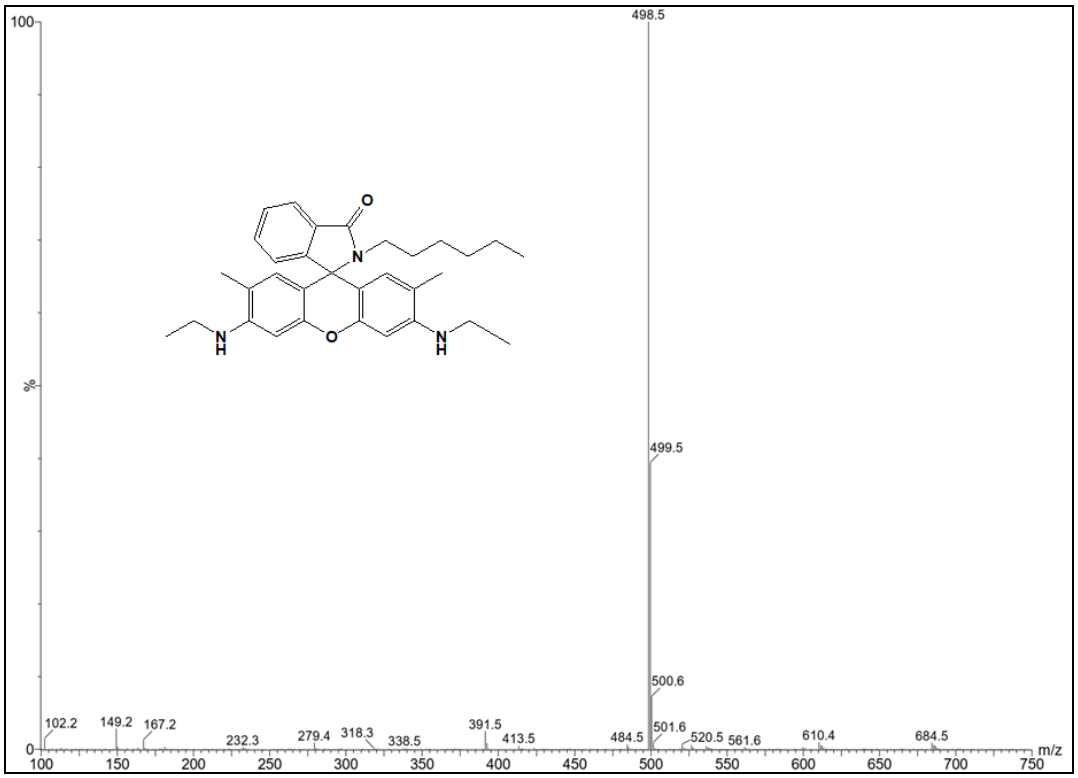

Fig. S16: MS (ESI) spectrum of compound **6**.

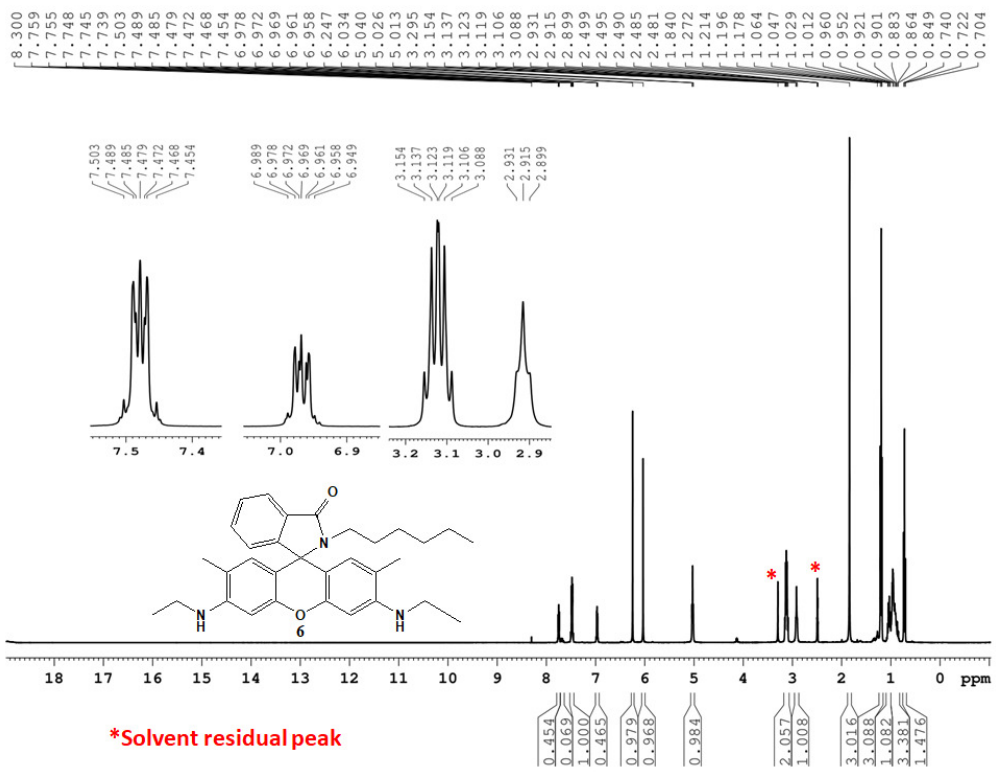

Fig. S17: ^{1}H NMR spectrum of compound **6** (in DMSO-d_6)

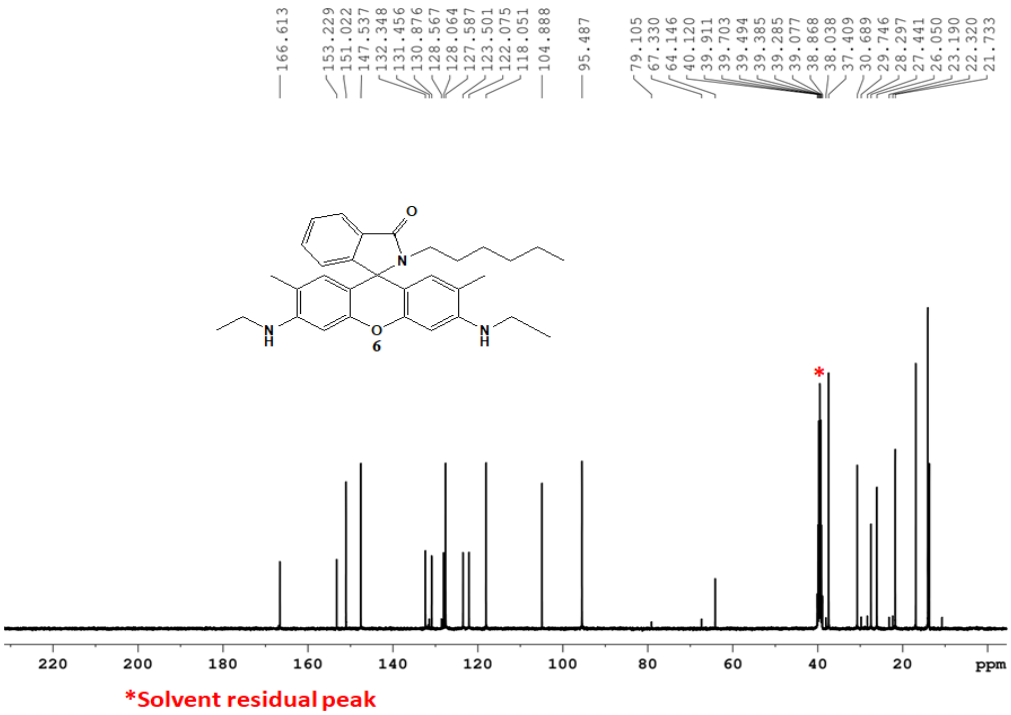

Fig. S18: ^{13}C NMR spectrum of compound **6** (in DMSO-d_6).

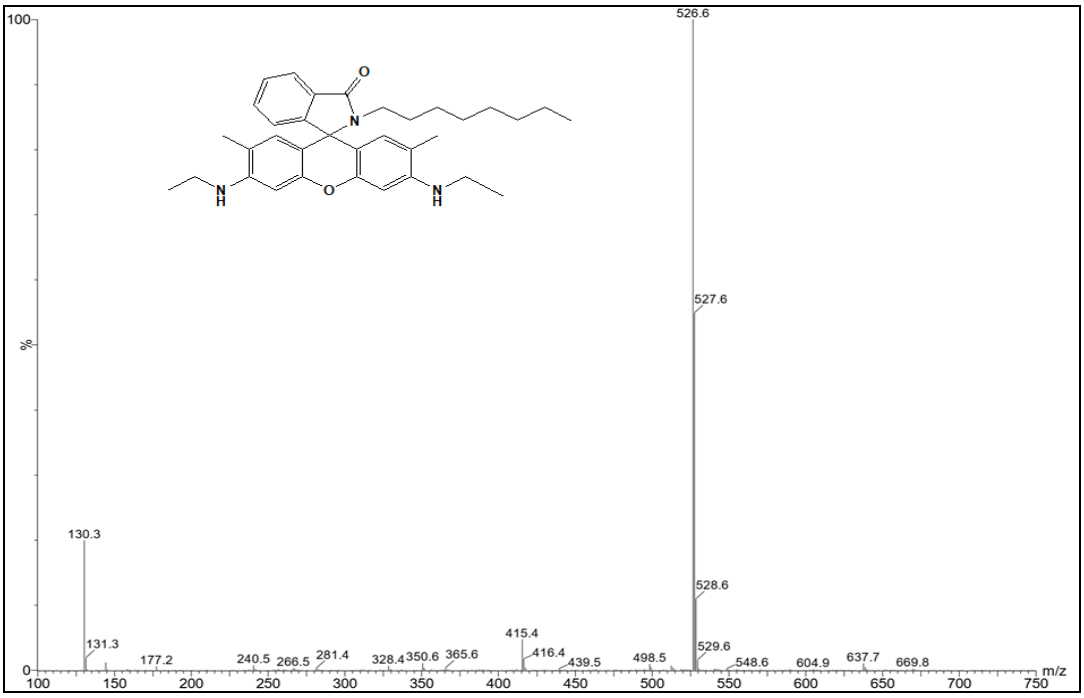

Fig. S19: MS (ESI) spectrum of compound **7**.

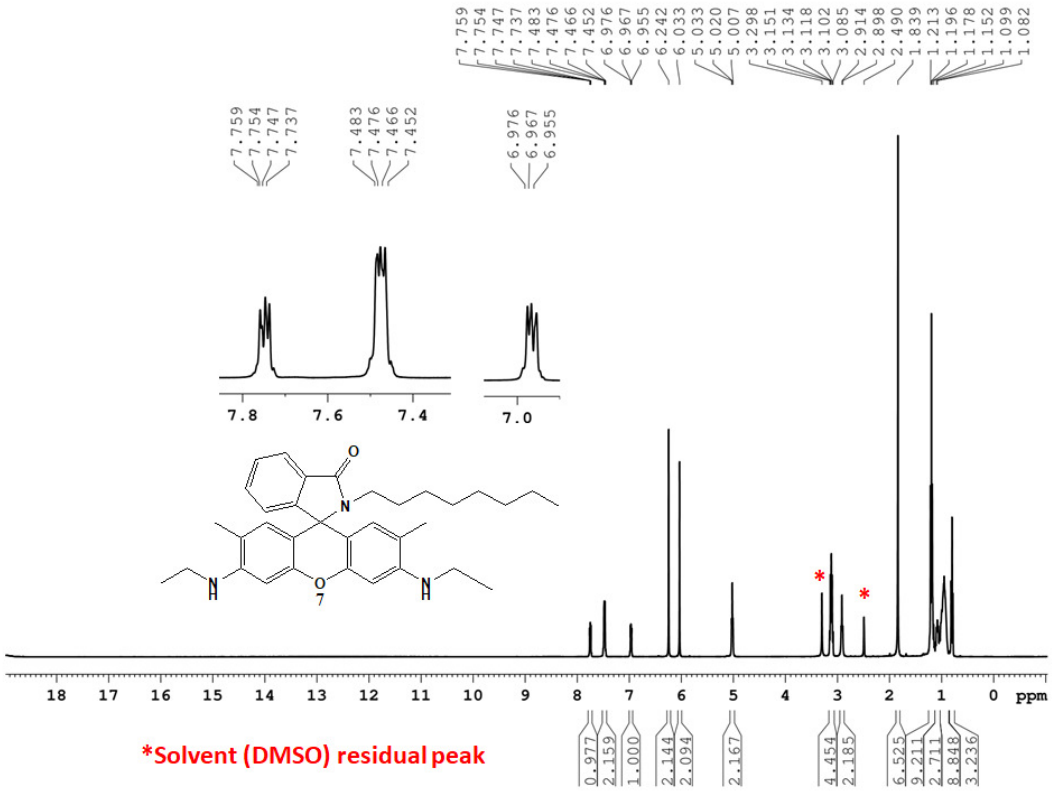

Fig. S20: ^{1}H NMR spectrum of compound **7** (in DMSO-d_6)

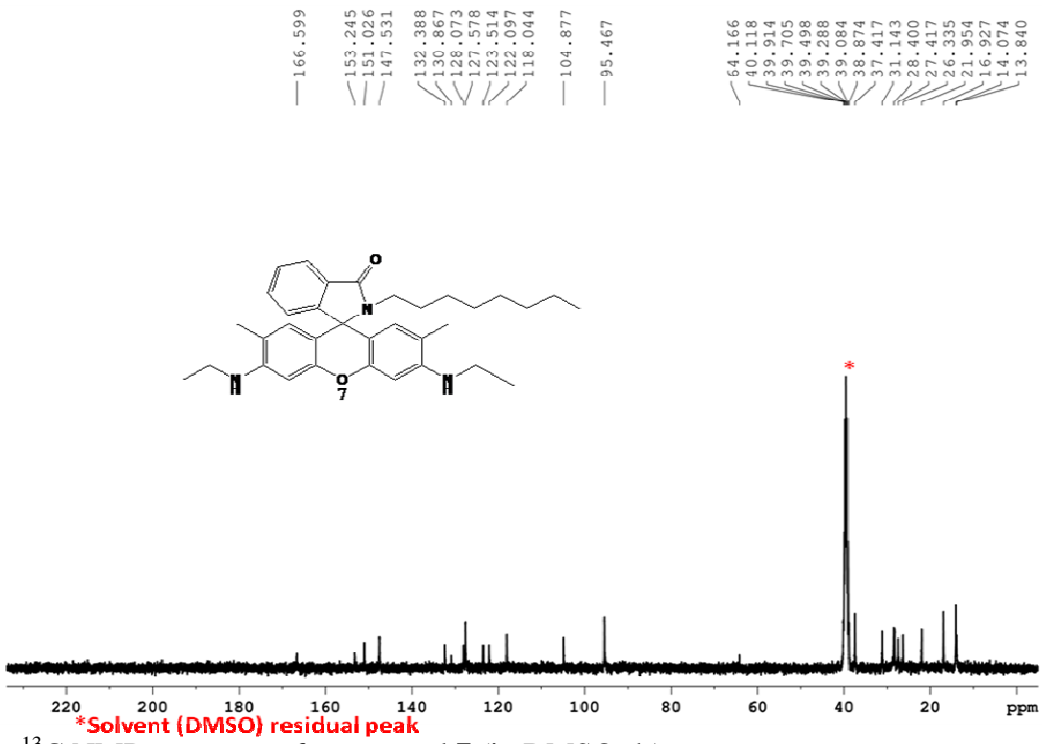

Fig. S21: ^{13}C NMR spectrum of compound **7** (in DMSO-d_6).

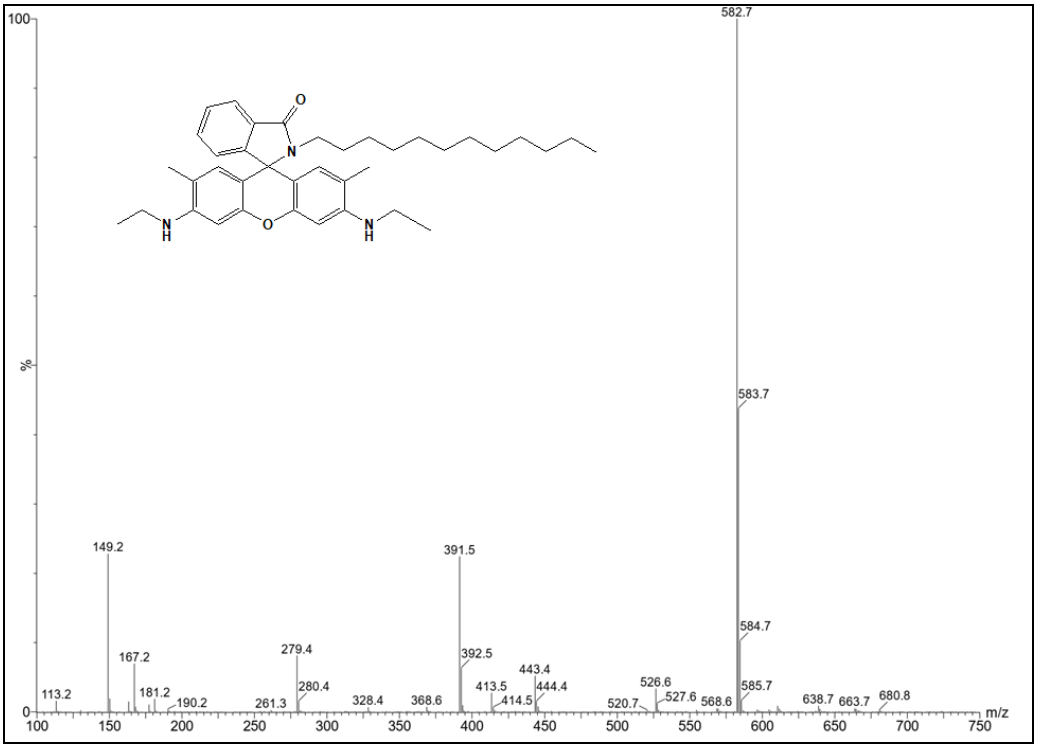

Fig. S22: MS (ESI) spectrum of compound **8**.

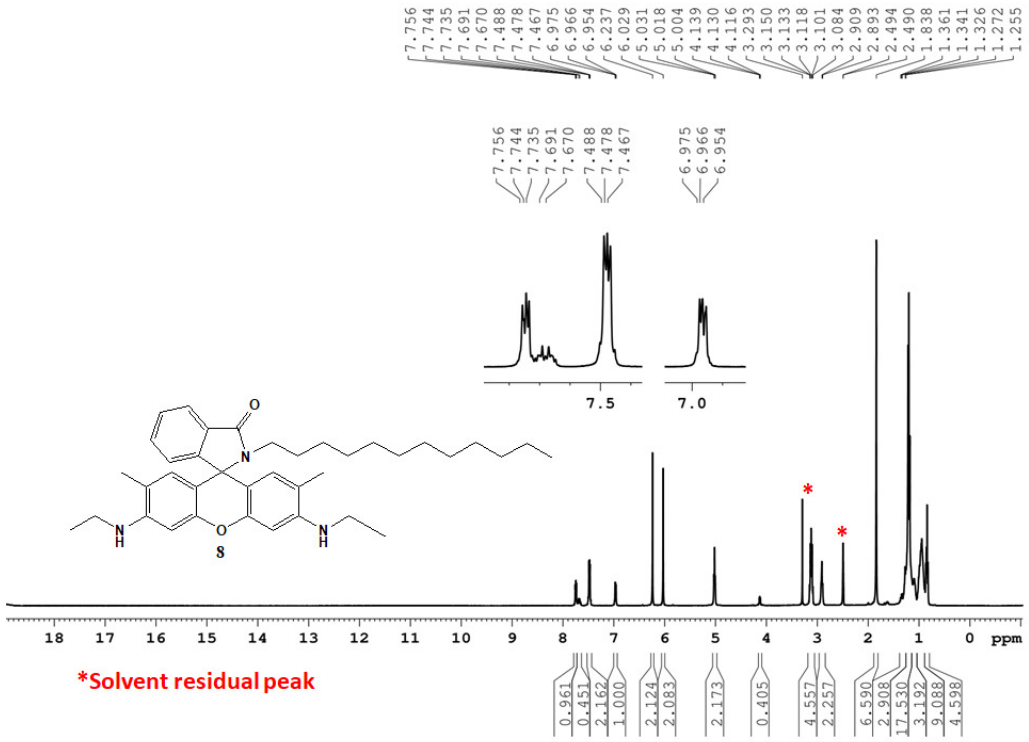

Fig. S23: ^{1}H NMR spectrum of compound **8** (in DMSO-d_6)

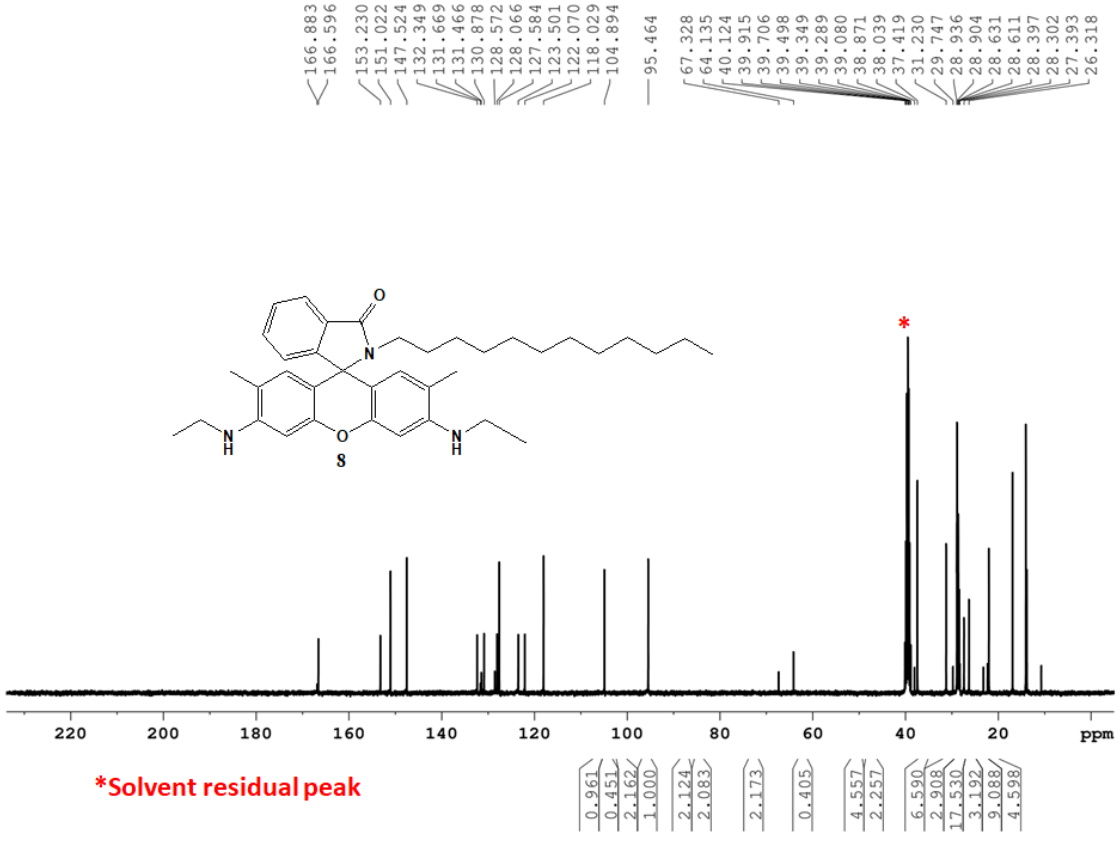

Fig. S24: ^{13}C NMR spectrum of compound **8** (in DMSO-d_6).

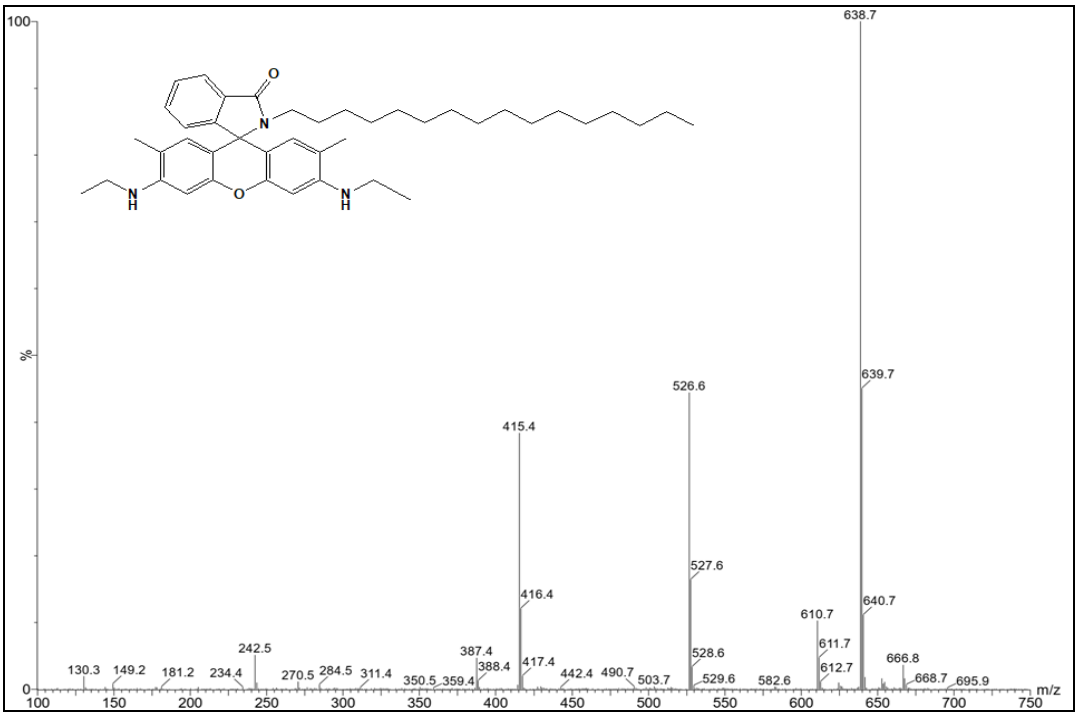

Fig. S25: MS (ESI) spectrum of compound **9**.

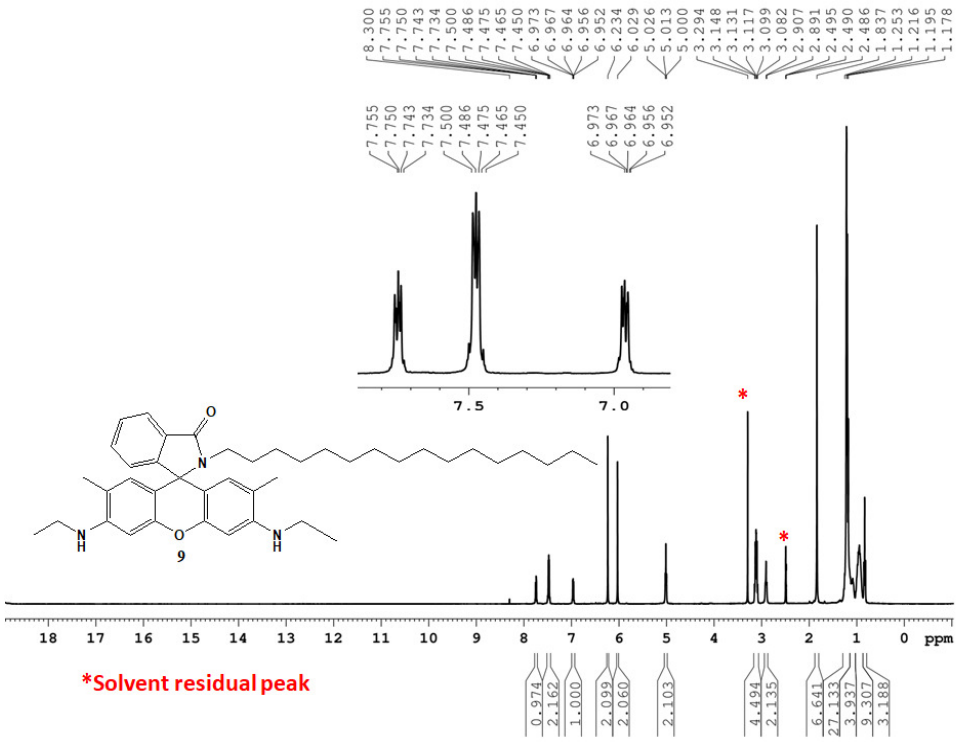

Fig. S26: ^{1}H NMR spectrum of compound **9** (in DMSO-d_6)

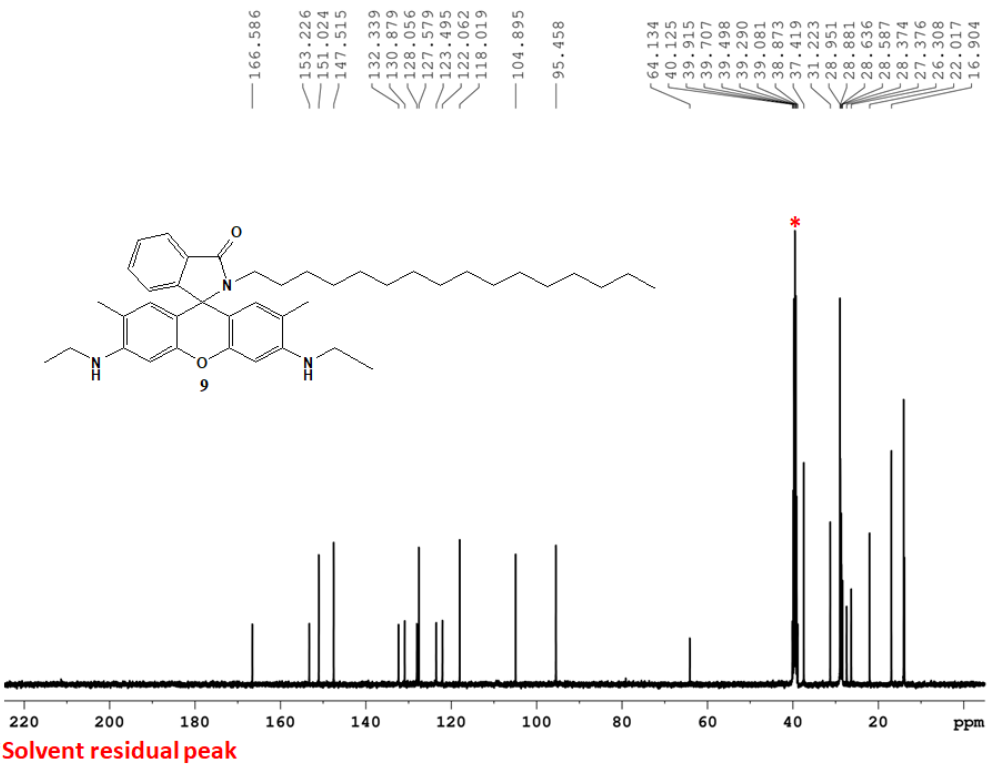

Fig. S27: ^{13}C NMR spectrum of compound **9** (in DMSO-d_6).

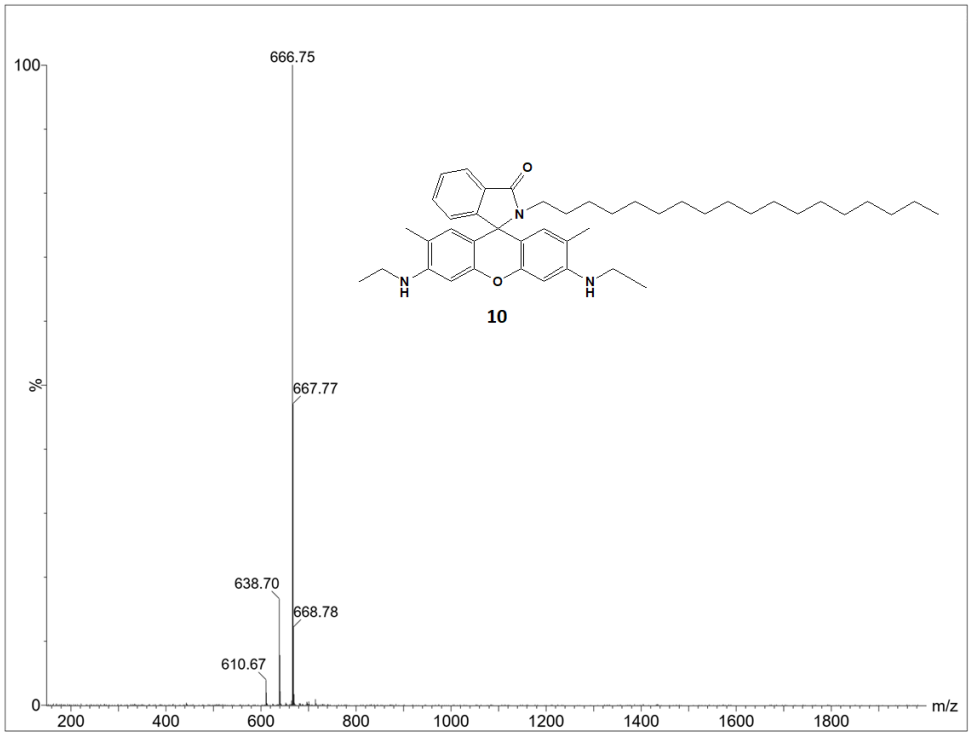

Fig. S28: MS (ESI) spectrum of compound **10**.

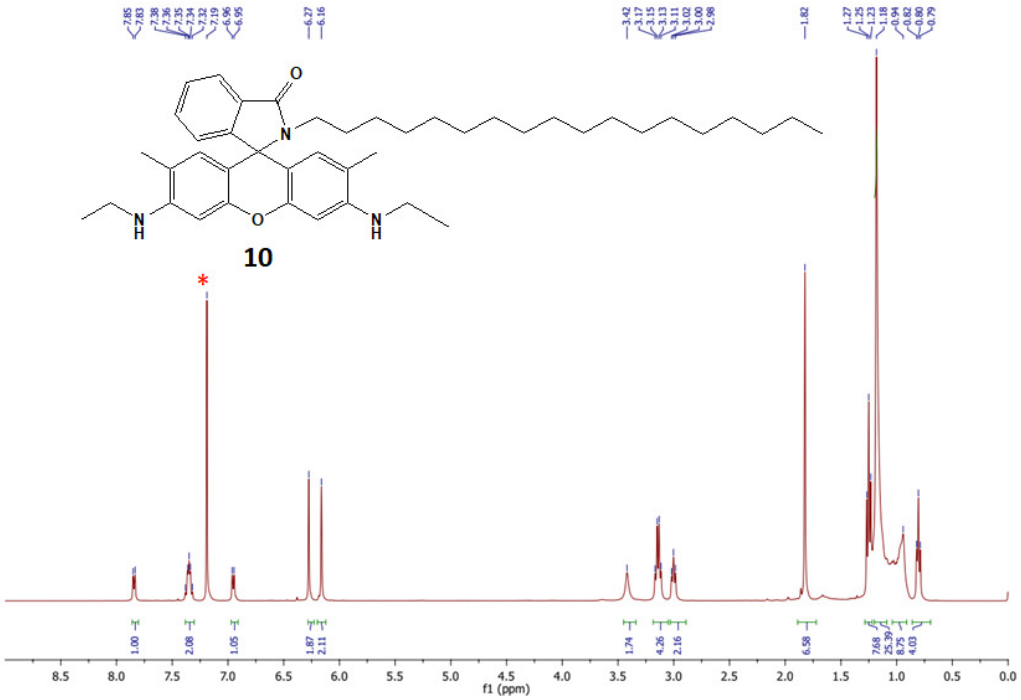

Fig. S29: ^{1}H NMR spectrum of compound **10** (in $CDCl_3$).

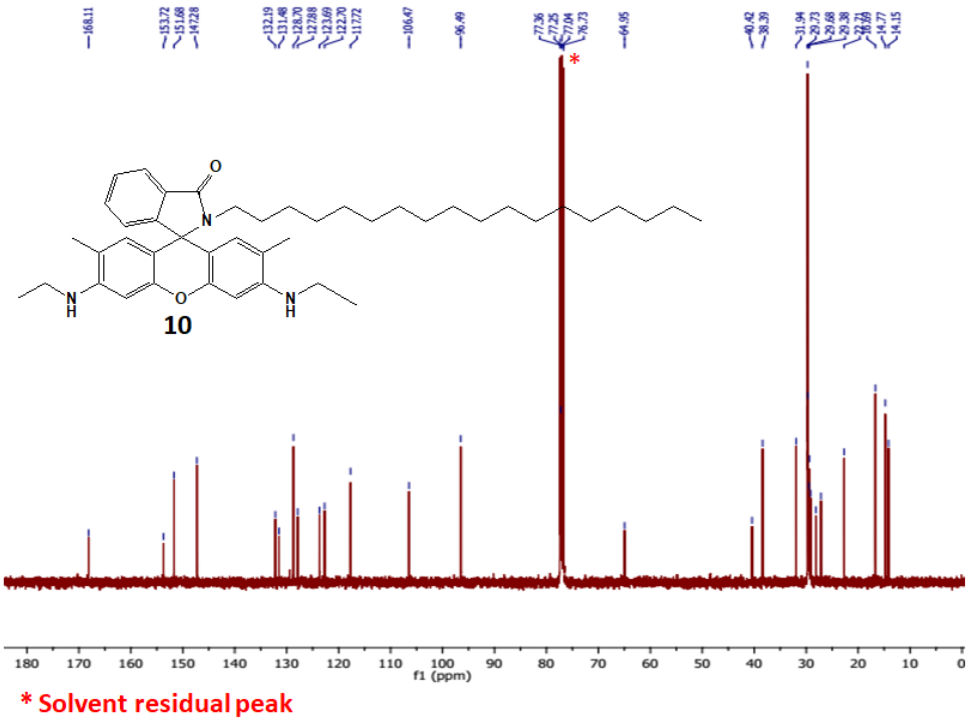

Fig. S30: ^{13}C NMR spectrum of compound **10** (in $CDCl_3$).

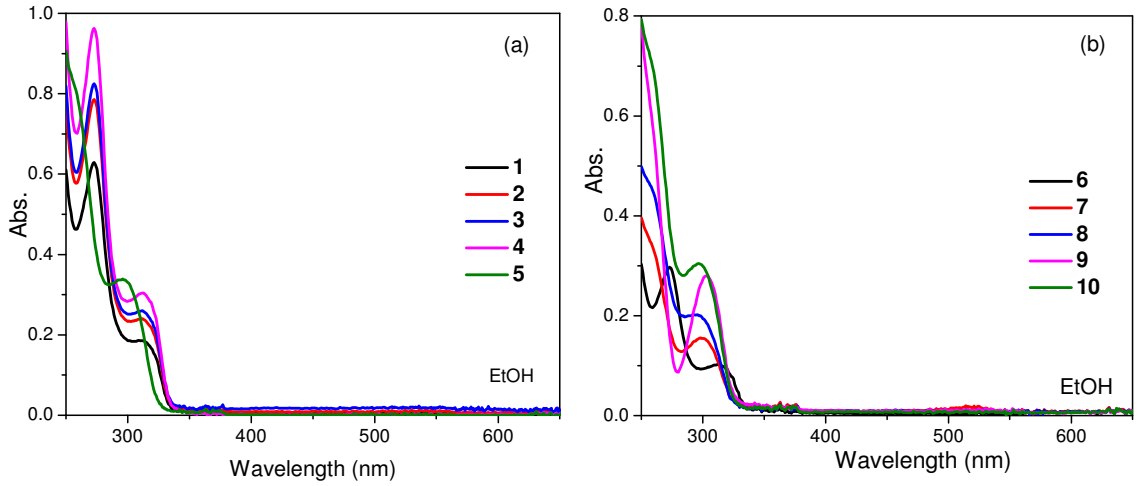

Fig. S31: Absorption spectra of (a) **1**-**5** and (b) **6**-**10** in EtOH. Conditions: [probe] =10 μM.

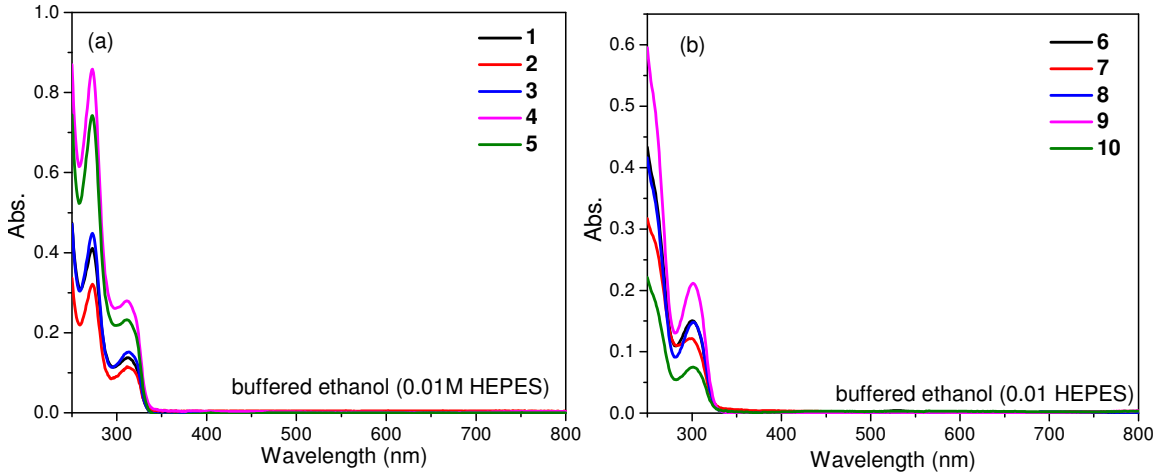

Fig. S32: Absorption spectra of (a) **1**-**5** and (b) **6**-**10** in buffered EtOH; Cond^{n}: [probe] =10 μM.

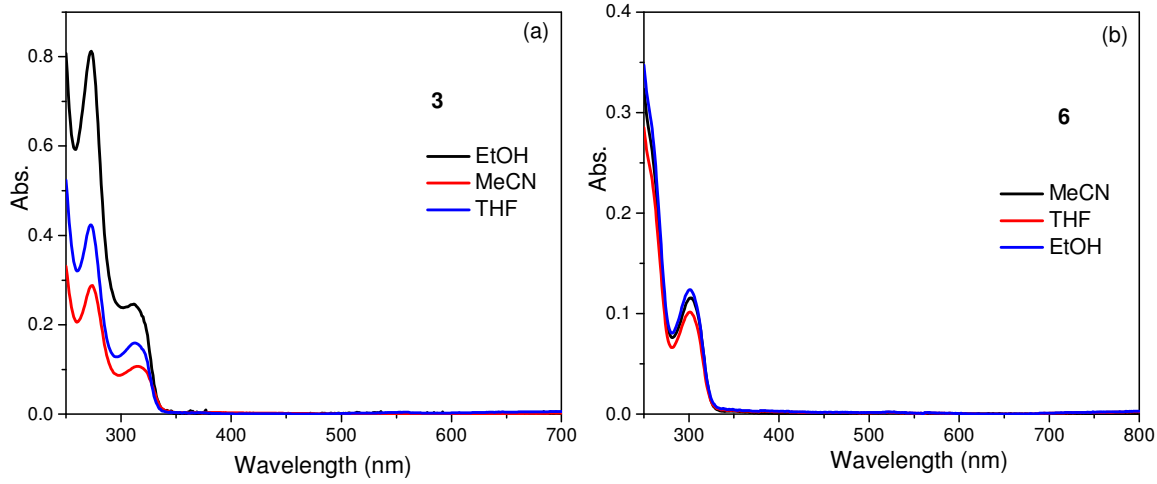

Fig. S33: Comparative absorption spectra of (a) **3** and (b) **6** in different organic solvents medium. Conditions: [**3**, **6**] =10 μM.

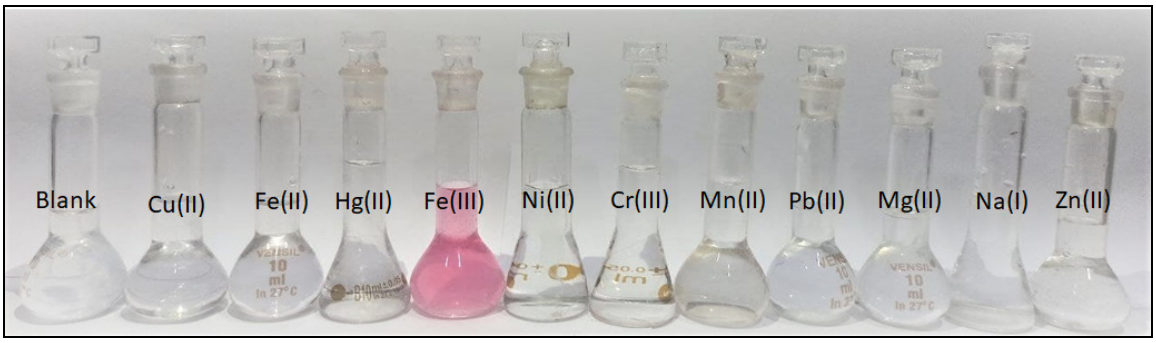

Fig. S34: Photograph depicting colorimetric sensing of **1** in presence of various metal ions in EtOH-H_2O (0.01 M HEPES, 9:1 v/v) medium. [**1**] = 10µM, [M(I/II/III)] = 100µM.

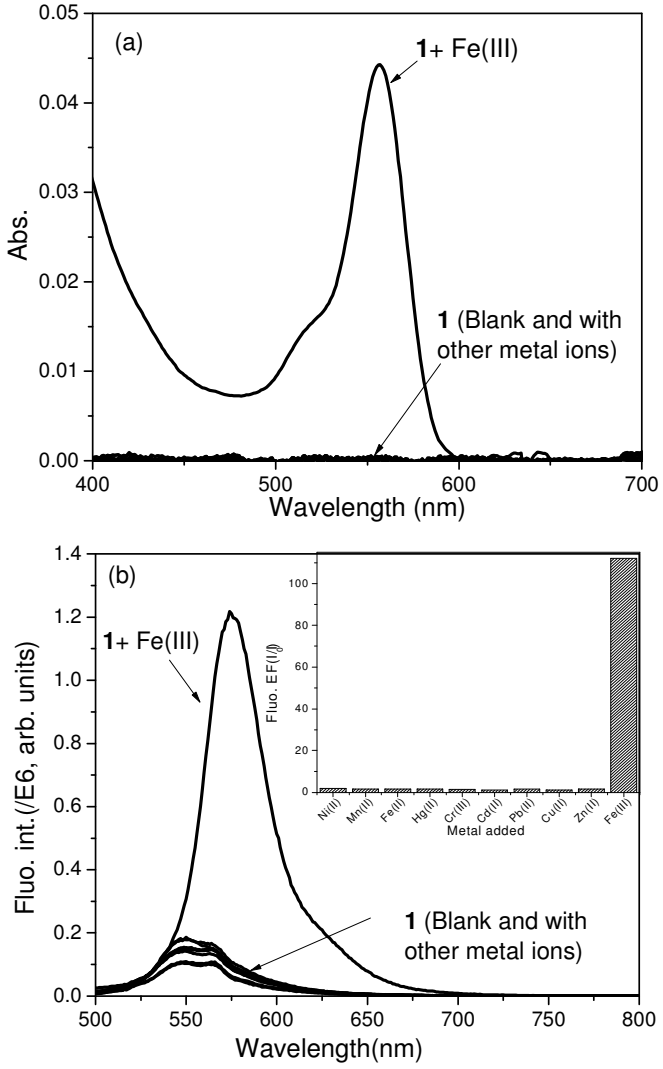

Fig. S35: Absorption (a) and steady-state fluorescence (b) spectra of **1** alone and in presence of various metal ions in EtOH-H_2O (0.01 M HEPES, 9:1 v/v). Conditions: Abs.: [**1**]=10µM, [M(I/II/III)]=50 µM. Fluo.: [**1**]= 1 µM, [M(I/II/III)] = 10µM, λ_{ex}= 500 nm, ex. /em. b. p. = 5 nm.

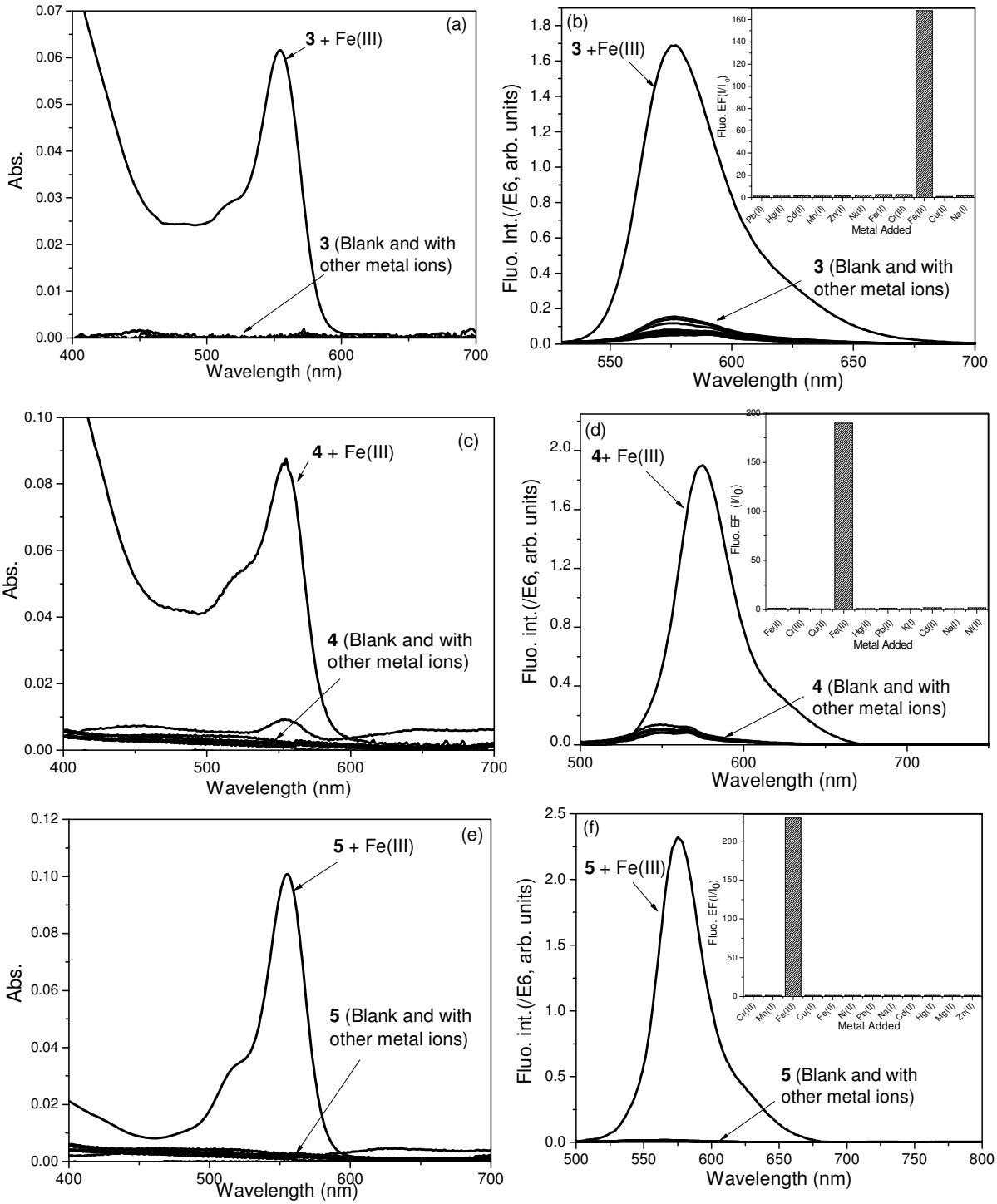

Fig. S36: Absorption (a, c, e) and steady-state fluorescence spectra (b, d, f) of **3**, **4**, **5** alone and in presence of various metal ions in EtOH-H_2O (0.01 M HEPES, 9:1 v/v) medium. Conditions: Abs.: [**3**, **4**, **5**] = 1×10^{-5} M, [M(I/II/III)] =1×10^{-4} M in all the cases. Fluo.: [**3**, **4**, **5**] = 1×10^{-6} M, [M(I/II/III)] = 1×10^{-5} M, λ_{ex}=500nm, RT, ex. and em. b. p. = 5 nm

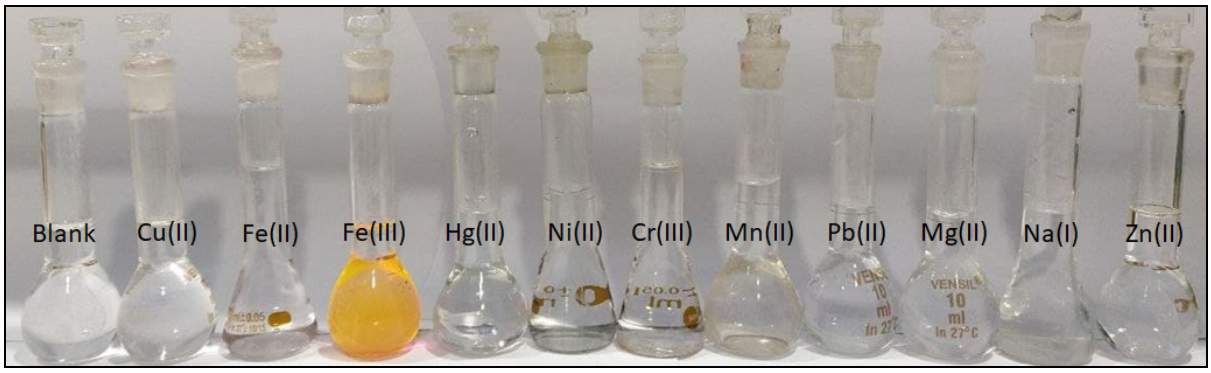

Fig. S37: Photograph depicting colour change of the solution of **6** with different metal ions in EtOH-H_2O (0.01 M HEPES, 9:1 v/v) medium. [**6**] = 10 μM, [M(I/II/III)] = 100 μM.

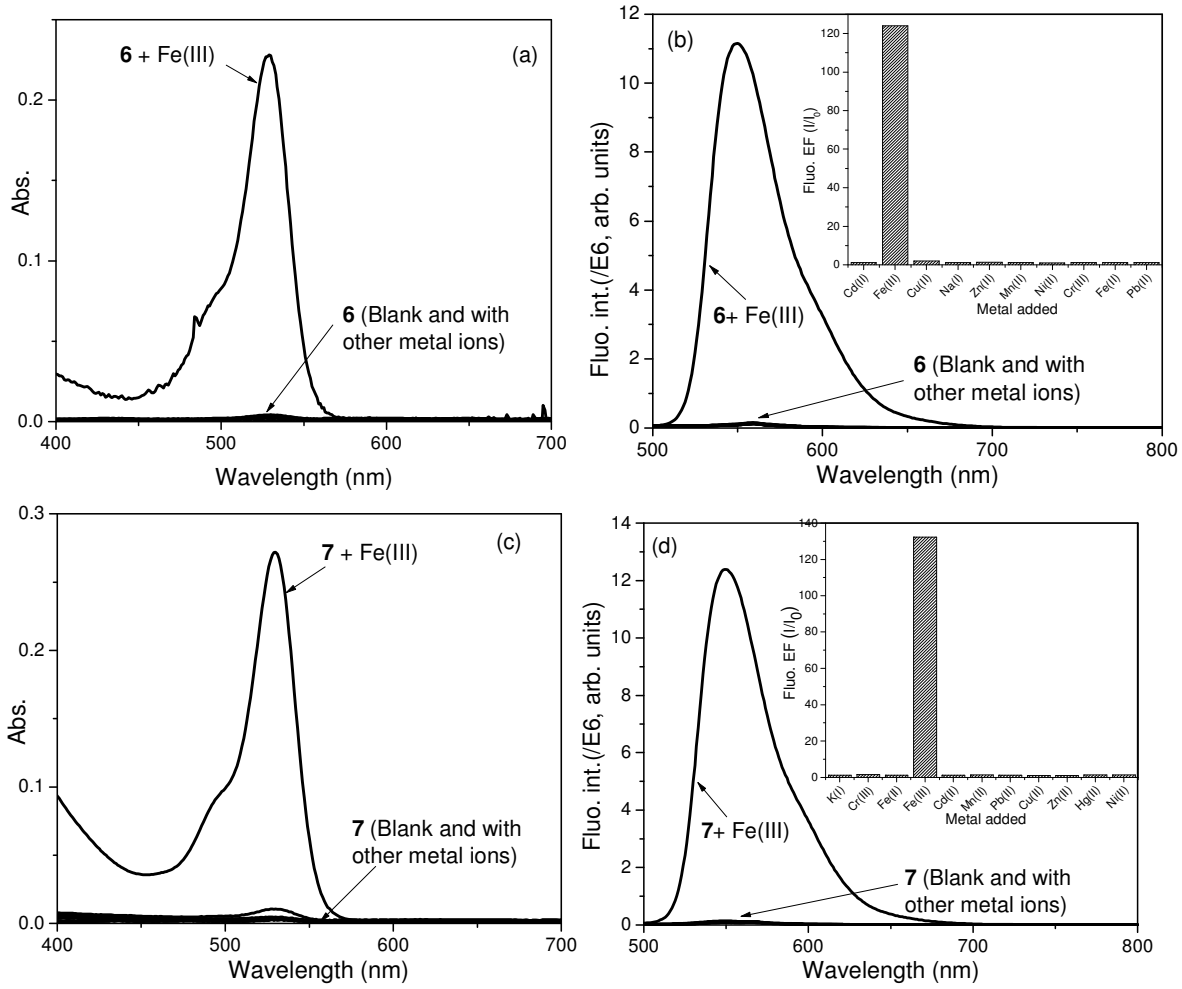

Fig. S38: Absorption (a) and steady-state fluorescence (b) spectra of **6** and **7** alone and in presence of various metal ions in EtOH-H_2O (0.01 M HEPES, 9:1 v/v) medium. Conditions: Abs.: [**7**] = 1×10^{-5} M, [M(I/II/III)] =1×10^{-4} M in all the cases. Fluo.: [**7**] = 1×10^{-6} M, [M(I/II/III)] = 1×10^{-5} M, λ_{ex}= 500 nm, RT, ex. and em. b. p. = 5 nm.

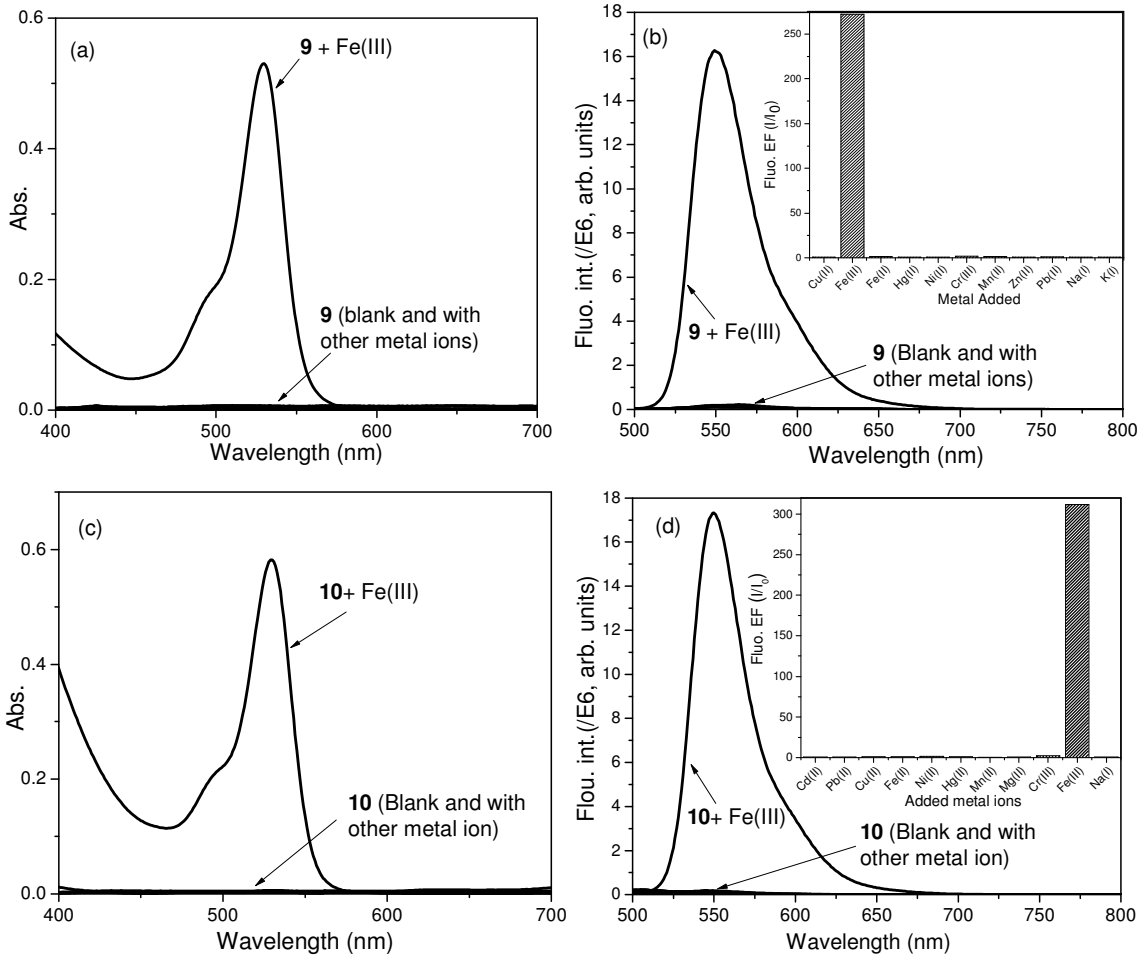

Fig. S39: Absorption (a, c) and steady-state fluorescence spectra (b, d) of **9** (a, b) and **10** (c, d) alone and in presence of various metal ions in EtOH-H_2O (0.01 M HEPES, 9:1 v/v) medium. Conditions: Abs.: [**9**, **10**] = 1×10^{-5} M, [M(I/II/III)] =1×10^{-4} M. Fluo.: [**9**, **10**] = 1×10^{-6} M, [M(I/II/III)] = 1×10^{-5} M, λ_{ex}=500 nm, RT, ex. and em. b. p. = 5 nm.

Table ST1: Fit-results to the exponential decay curve of **1**-**3** with and without Fe(III) ions, obtained with time-correlated single photon counting technique which were best-fitted to the bi-exponential fit equation $A+B_1 \exp(-t/\tau_1) + B_2 \exp(-t/\tau_2)$.

Parameters	**1**	**1** + Fe(III)	**2**	**2** + Fe(III)	**3**	**3** + Fe(III)
τ_1, ns (Rel %)	2.35 (92.96)	2.49 (94.45)	2.29 (94.08)	2.59 (95.84)	2.27 (92.92)	2.57 (96.23)
τ_2, ns (Rel %)	0.13 (7.04)	0.149 (5.55)	0.14 (5.92)	0.22 (4.16)	0.13 (7.08)	0.19 (3.77)
B1	5193.180	5392.744	5582.376	5661.601	4883.592	5510.361
B2	75.383	49.808	61.777	24.682	72.169	25.466
A	9.318	7.842	9.075	7.124	9.886	7.484
χ^2	1.267	1.136	1.249	1.254	1.108	1.157

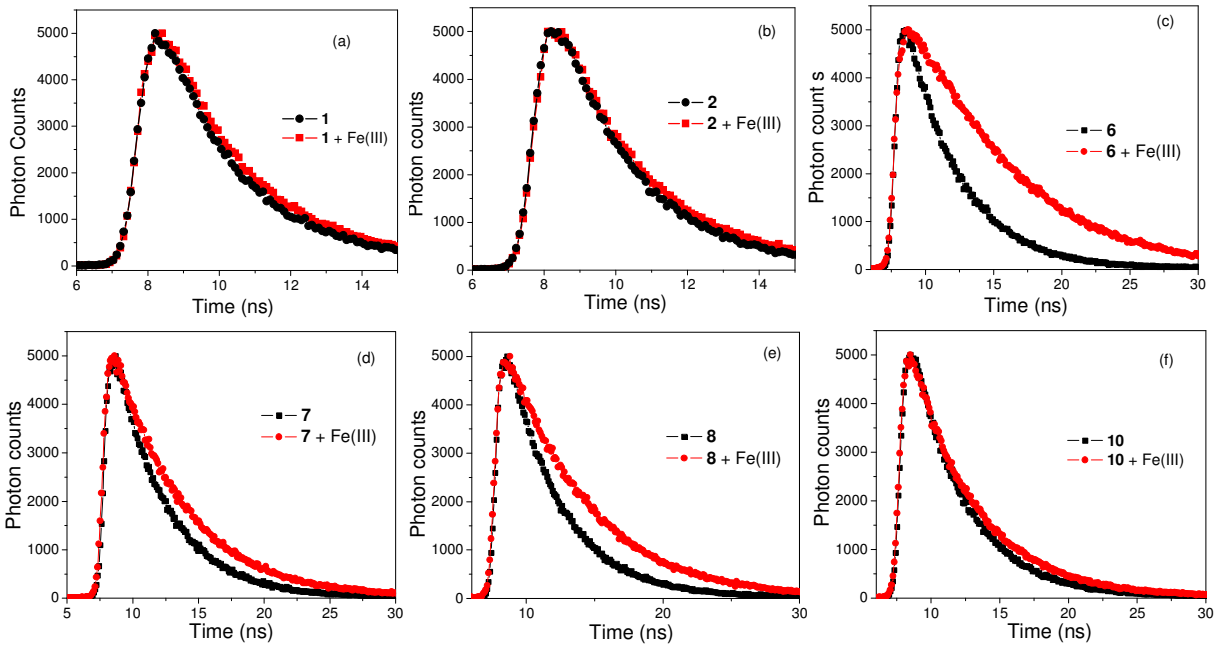

Fig. 40: (a) Fluorescence decay (TCSPC) profile of few probes alone and in presence of Fe(III) (1:1 stoichiometry) in EtOH-H_2O (0.01M HEPES, 9:1 v/v) medium. [L] = 1 μM, λ_{ex} = 480 nm, λ_{em} = 580 nm.

Table ST2: Fit-results to the exponential decay curve of **6-10** with and without Fe(III) ions, obtained with time-correlated single photon counting technique which were best-fitted to the bi-exponential fit equation $A+B_1 \exp(-t/\tau_1) + B_2 \exp(-t/\tau_2)$.

Parameters	**6**	**6**+Fe(III)	**7**	**7**+Fe(III)	**8**	**8**+Fe(III)	**10**	**10**+Fe(III)
τ_1, ns (Rel %)	3.83 (96.1)	7.21 (100)	3.88 (96.32)	5.29 (100)	3.86 (95.95)	5.76 (89.16)	3.88 (96.49)	4.62 (96.83)
τ_2, ns (Rel %)	0. 22 (3.93)	-	0.22 (3.68)	2.00 (0.00)	0.27 (4.05)	0.05 (10.84)	0.23 (3.51)	0.22 (3.17)
B1	5177.809	5655.364	5026.653	0.000	5173.701	5053.483	5370.329	5119.308
B2	35.614	-	33.621	5107.912	31.317	22.786	32.615	34.378
A	12.400	24.970	11.609	17.708	10.647	4.447	11.990	13.310
χ^2	1.168	2.385	1.156	1.321	1.117	1.193	1.069	1.132

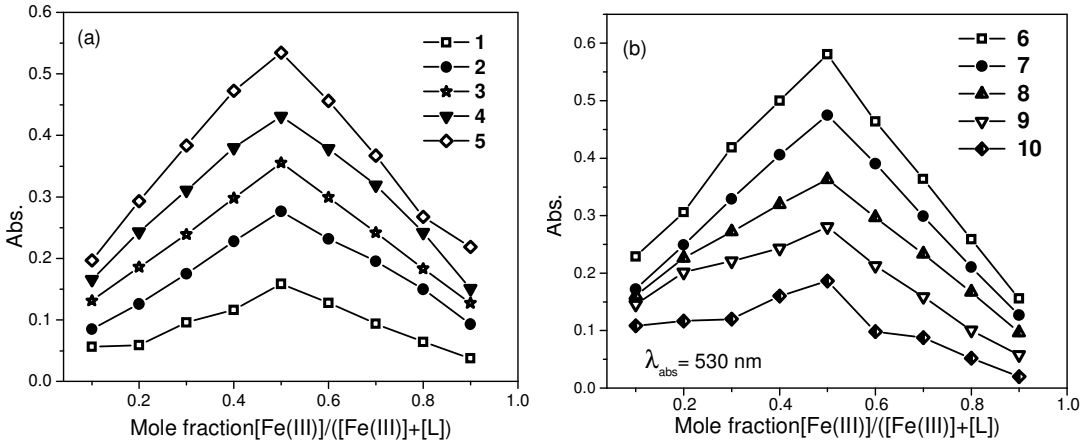

Fig. S41: Change in absorbance of these probes at their absorption maxima (λ_{abs} = 550 nm for **1**-**5** (a) and λ_{abs} = 530 nm for **6**-**10** (b)) as a function of mole fractions of added Fe(III) in EtOH-H_2O (0.01M HEPES, 9:1 v/v) showing 1:1 complexation stoichiometry (Job's plot).

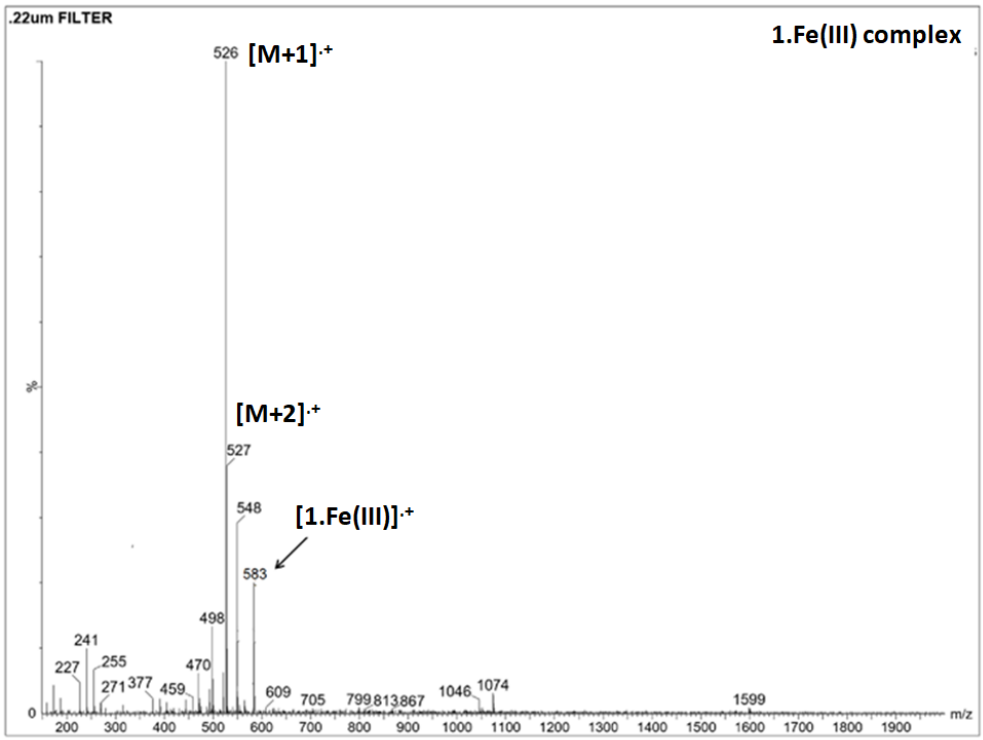

Fig. S42: MS (ESI) spectrum of **1**⊂Fe(III) complex.

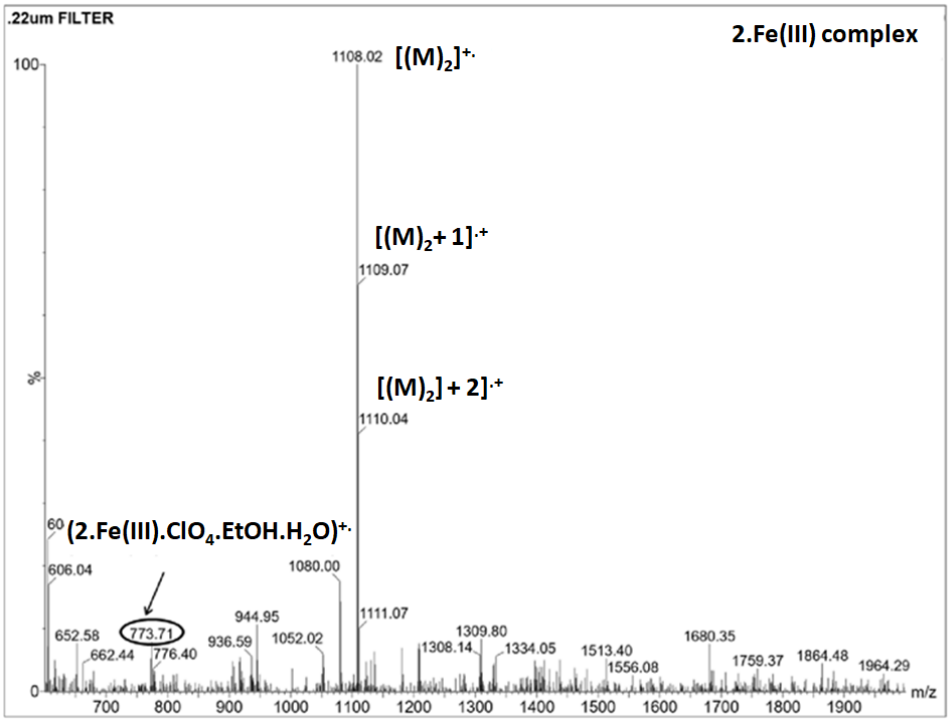

Fig. S43: MS (ESI) spectrum of **2**⊂Fe(III) complex.

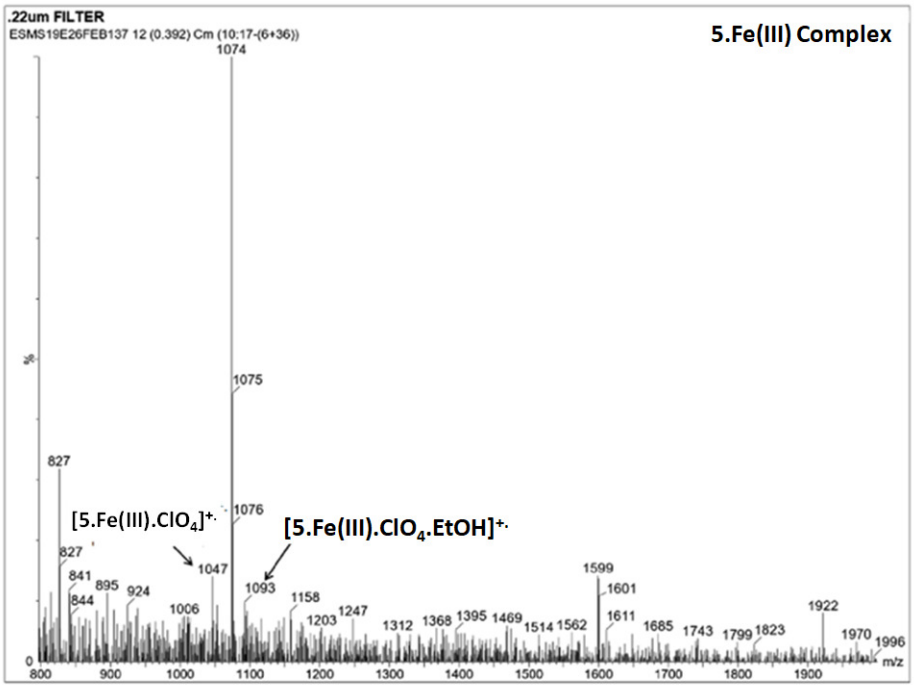

Fig. S 44: MS (ESI) spectrum of **5**⊂Fe(III) complex.

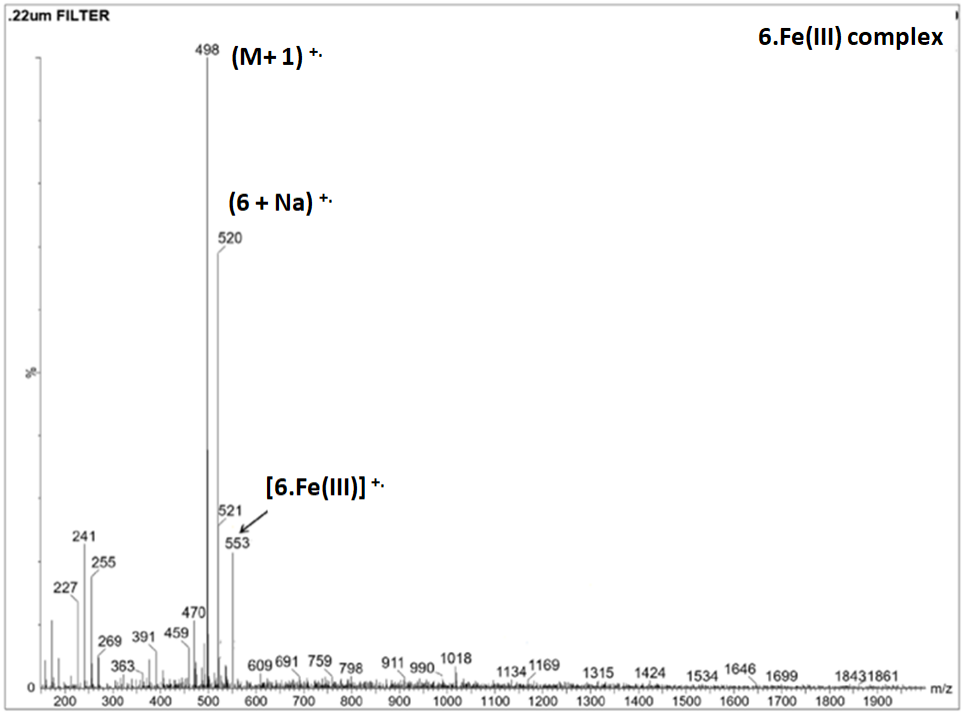

Fig. S45: MS (ESI) spectrum of **6**⊂Fe(III) complex

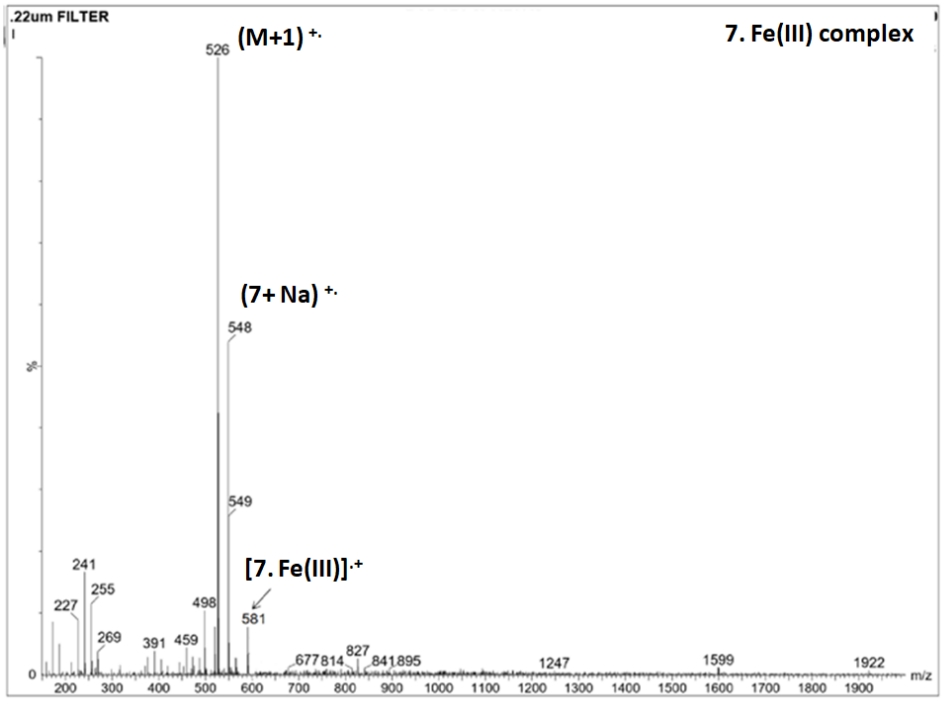

Fig. S46: MS (ESI) spectrum of **7**⊂Fe(III) complex.

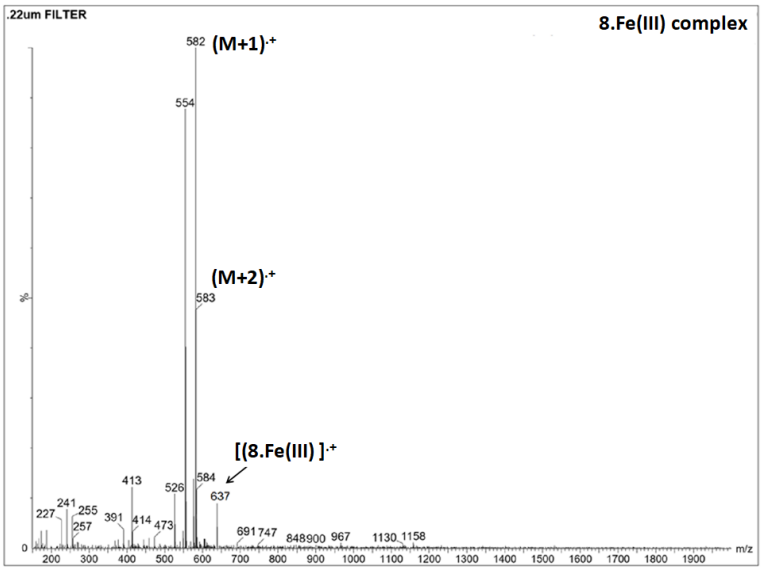

Fig. S47: MS (ESI) spectrum of **8**⊂Fe(III) complex.

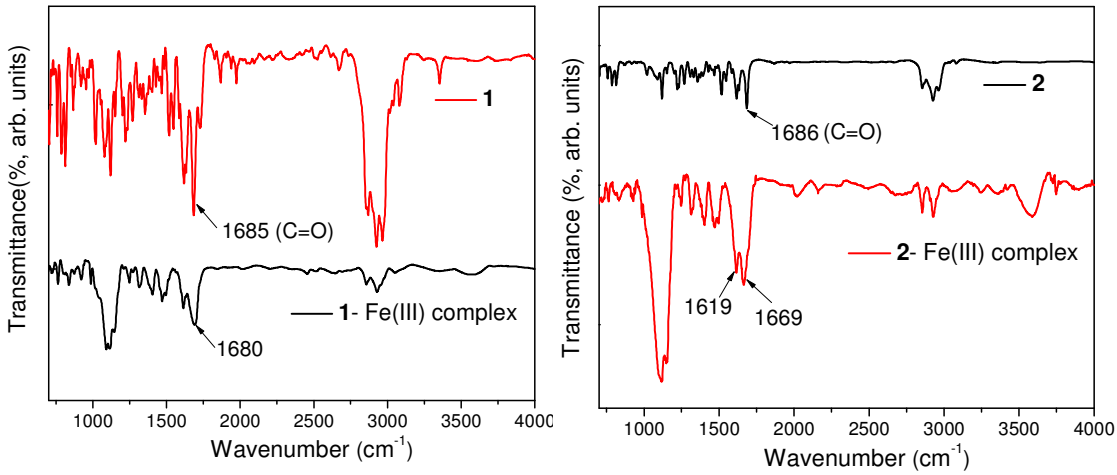

Fig. S48: FTIR-spectra of **1** and **2** with their corresponding Fe(III)-complexes (isolated solids).

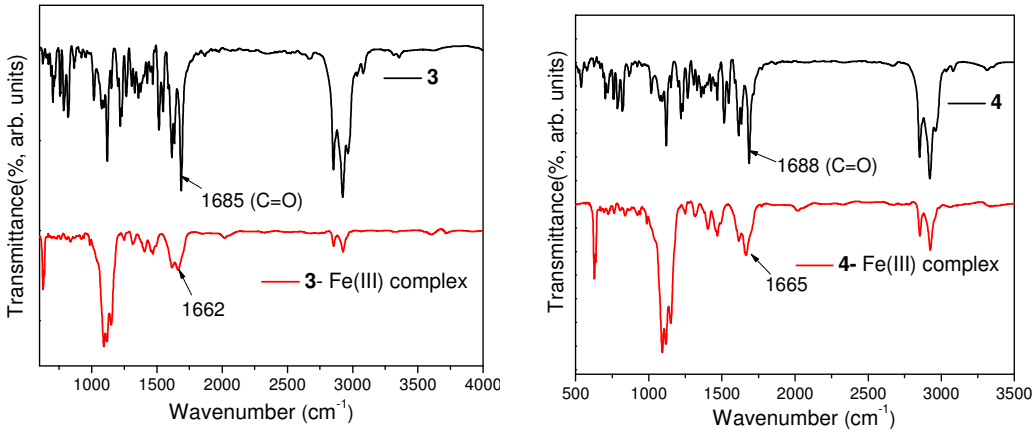

Fig. S49: FTIR-spectra of **3** and **4** with their corresponding Fe(III)-complexes (isolated solids).

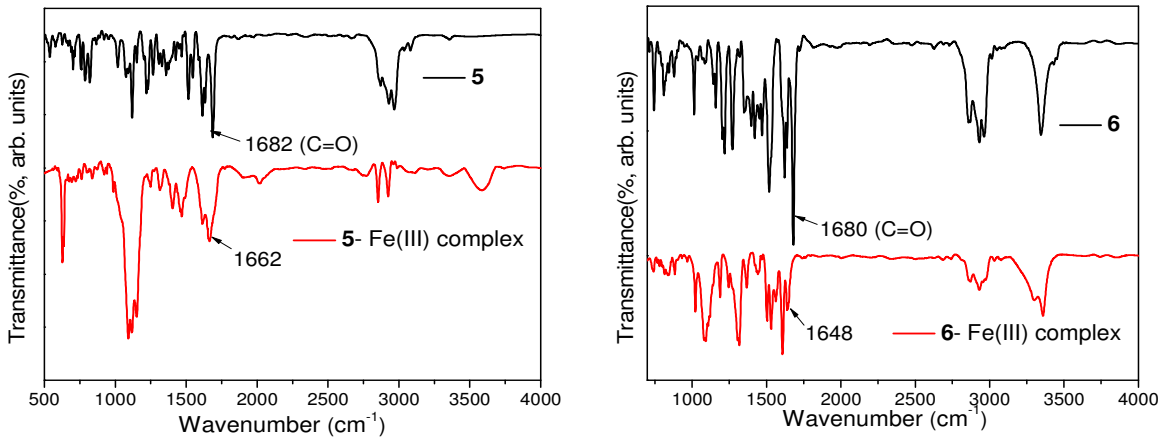

Fig. S50: Comparison between FTIR-spectra of **5** and **6** with their corresponding Fe(III)-complexes (isolated solids).

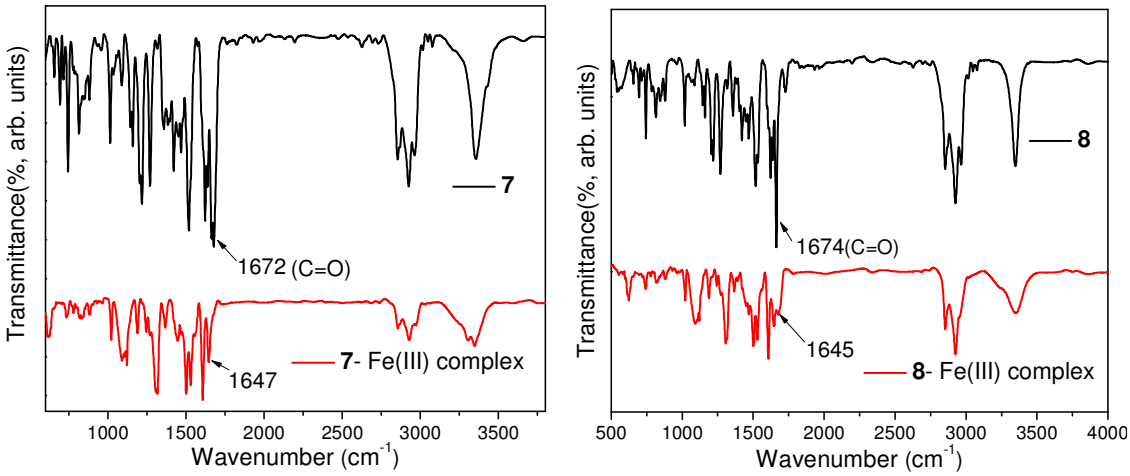

Fig. S51: Comparison between FTIR-spectra of **7** and **8** with those of their respective Fe(III)-complexes (isolated solids).

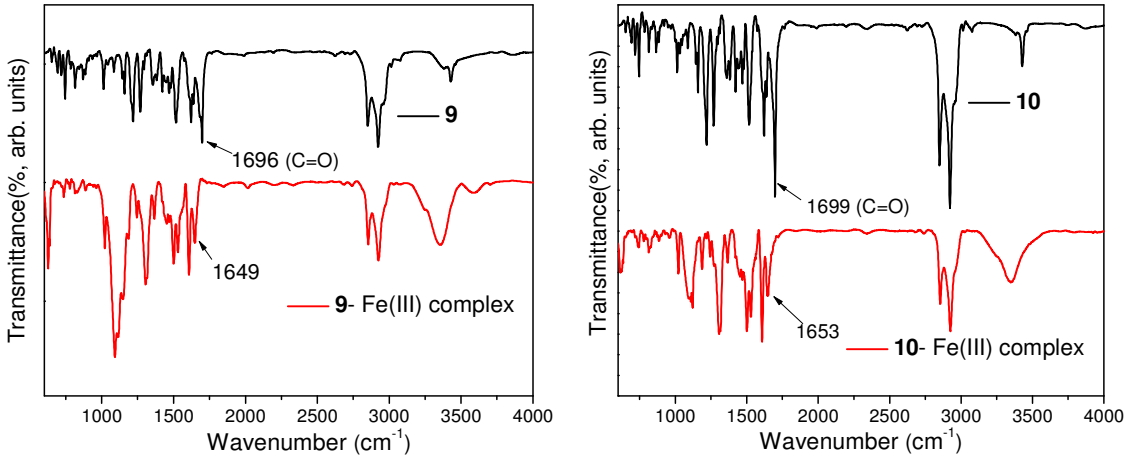

Fig. S52: Comparison between FTIR-spectra of **9** and **10** with those of their corresponding Fe(III)-complexes (isolated solids).

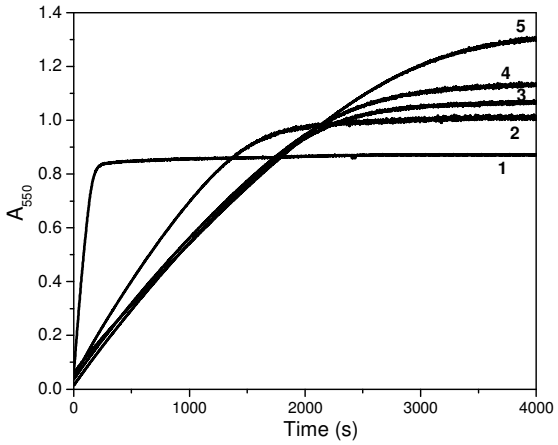

Fig. S53: Absorption spectral responses (λ_{abs}= 530 nm) of substituted Rhodamine B based probes (**1**-**5**) as a function of time (s) on addition of equimolar Fe(III) ion to probes' solutions.

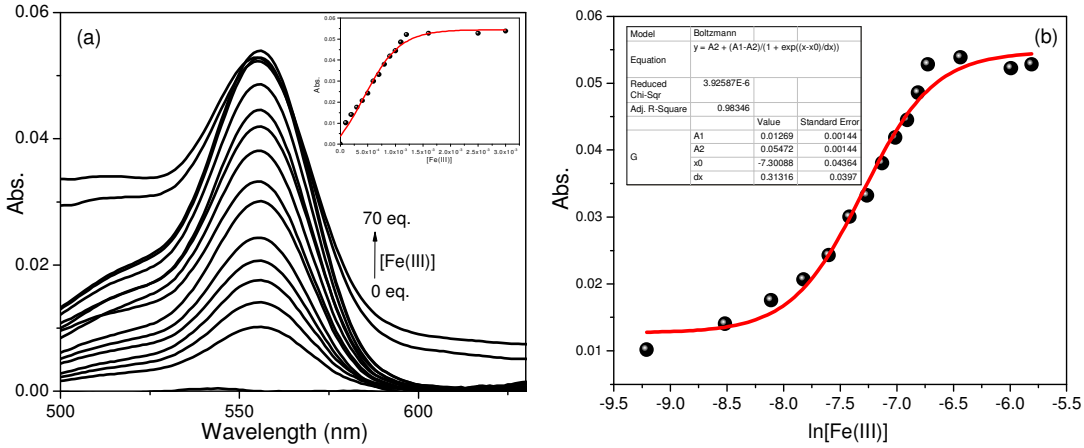

Fig. S54: (a) Absorption titrations of **1** with Fe(III) ions in EtOH-H_2O (0.01M HEPBS, 9:1 v/v) medium and (b) its corresponding intensity versus concentration (ln[Fe(III)] plots for determination of association constant (Ka). [**1**] = 1μM (abs.).

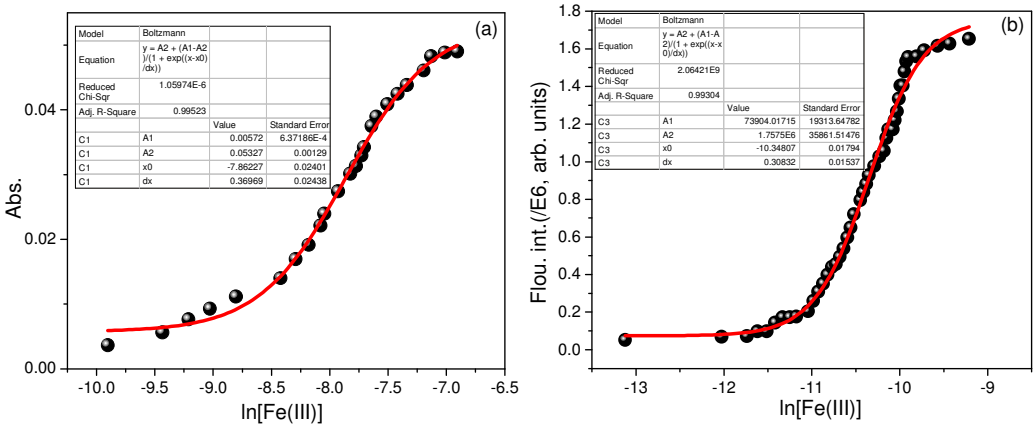

Fig. S55: Non-linear fit to the plot of (a) absorbance and (b) fluorescence of **2** as a function of concentrations of Fe(III) added (ln Fe(III)) for determination of association constant (Ka) of complexation. The graphs of absorption and fluorescence titrations are given in the main text.

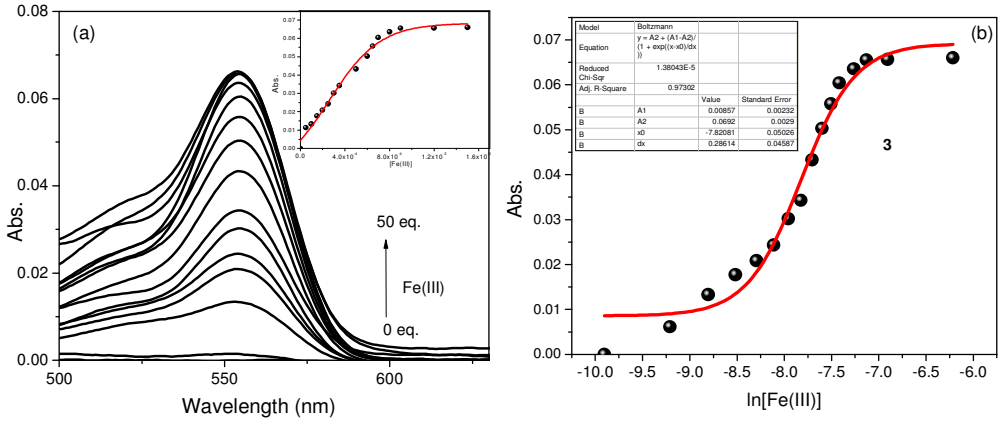

Fig. S56: (a) Absorption spectra of **3** in presence of Fe(III) ions in EtOH-H_2O (0.01M HEPBS, 9:1 v/v) medium, and (b) non-linear regression to the plot its corresponding intensity versus concentration (ln[Fe(III)] for determination of Ka. [**3**] = 1 μM (abs.).

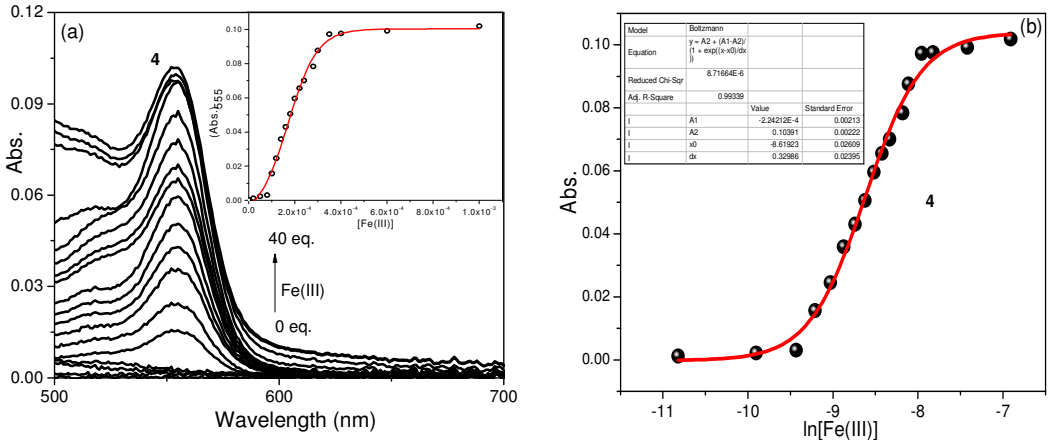

Fig. S57: (a) Absorption titrations of **4** with Fe(III) ions in EtOH-H_2O(0.01M HEPBS, 9:1 v/v), (b) non-linear regression to the plot of its corresponding intensity versus concentration (ln[Fe(III)] for determination of Ka. [**4**] = 1 μM (Abs.).

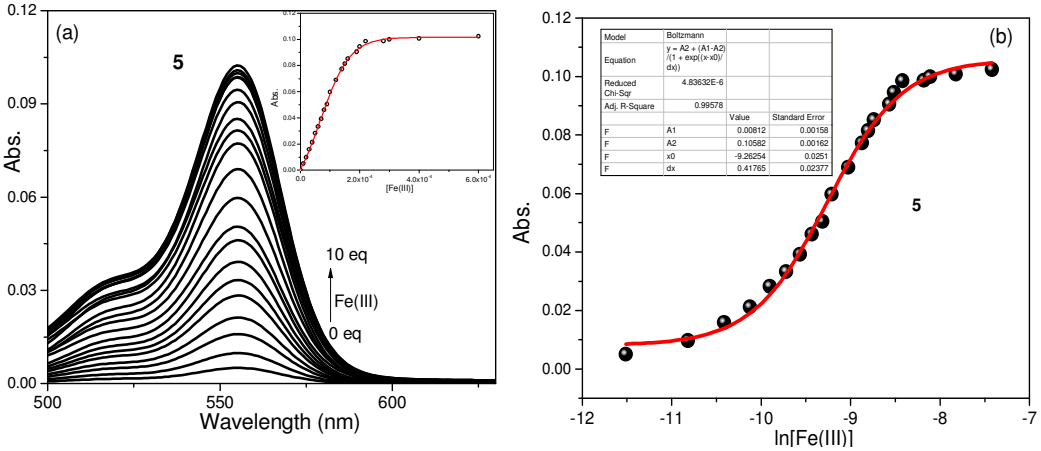

Fig. S58: (a) Absorption titrations of **5** with Fe(III) ions in EtOH-H_2O (0.01M HEPBS, 9:1 v/v), (b) non-linear regression to the plot of its corresponding intensity versus concentration (ln[Fe(III)] for determination of Ka. [**5**] = 1 μM (abs.).

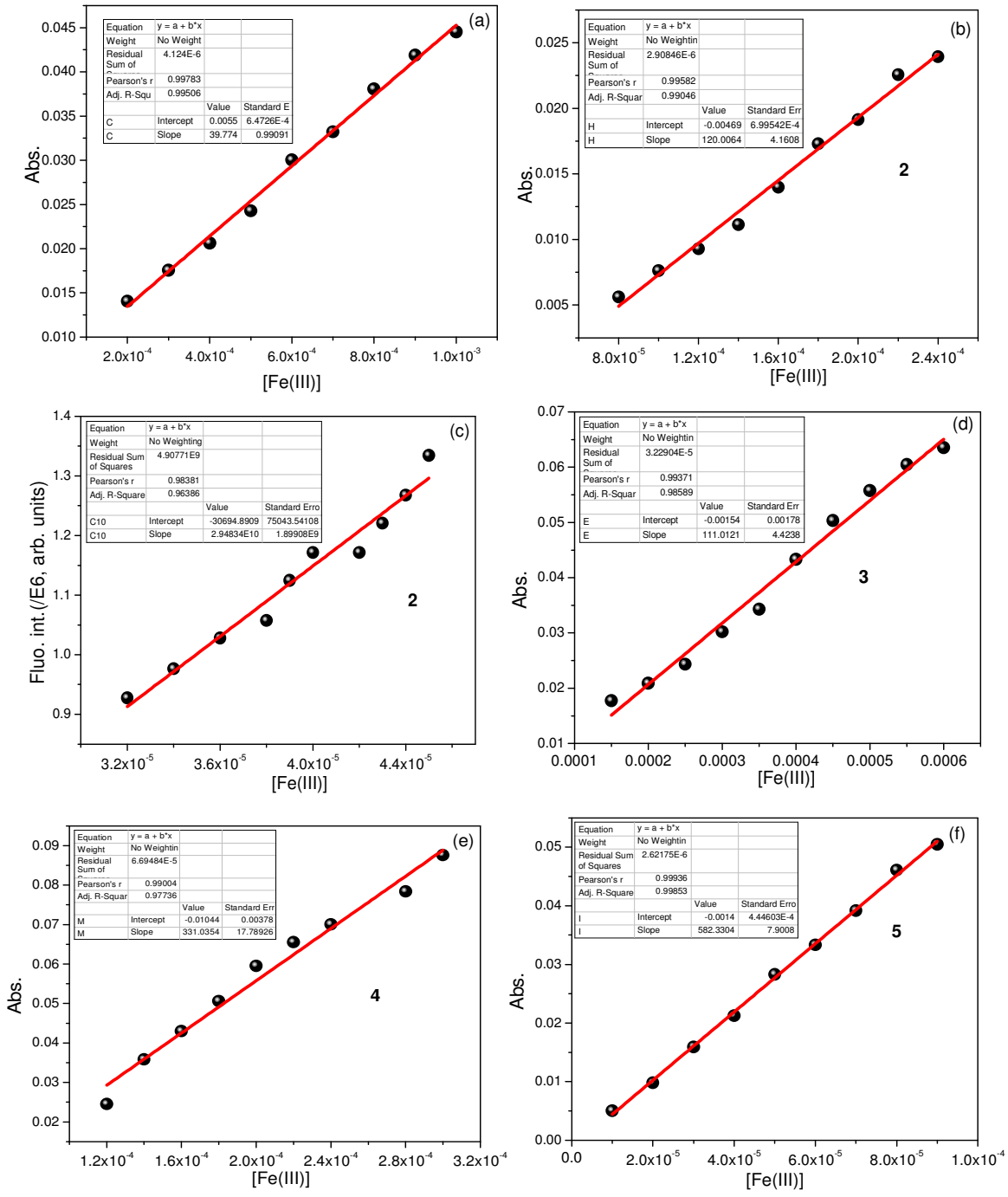

Fig. S59: Linear regression to the plot of absorbance of **1**, **2**, **3, 4** and **5** (a, b, d, e, and f, respectively) and fluorescence spectral intensities of **2** (c) on addition of added Fe(III) ion for determination of the sensitivity of detection (S/N=5).

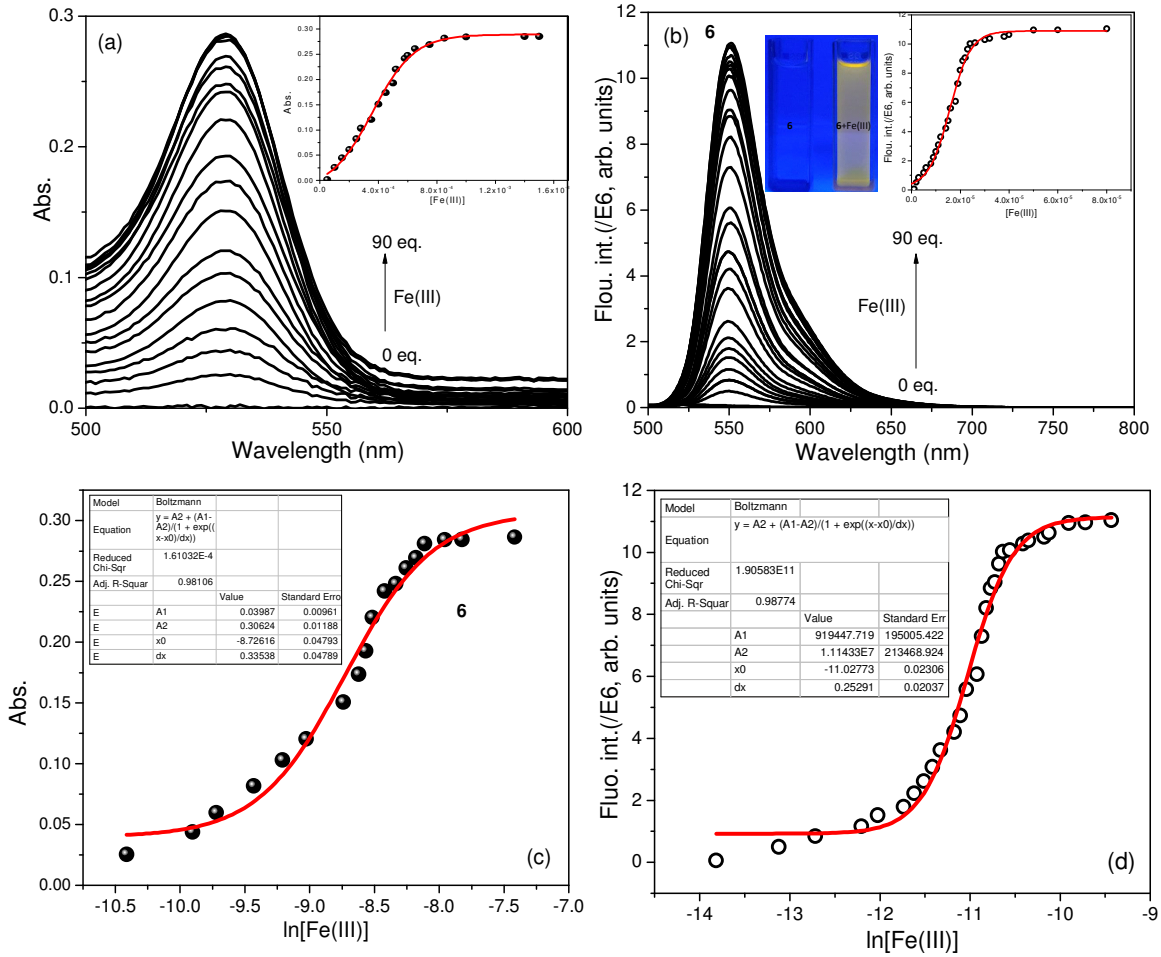

Fig. S60: (a) Absorption and (b) fluorescence spectra of **6** with added Fe(III) ions in EtOH-H_2O (0.01M HEPES, 9:1 v/v); (c and d) non-linear fit to the plot of its intensities versus concentration (ln[Fe(III)]) for determination of Ka. [**6**] = 10 μM (abs.); 1 μM (Fluo.).

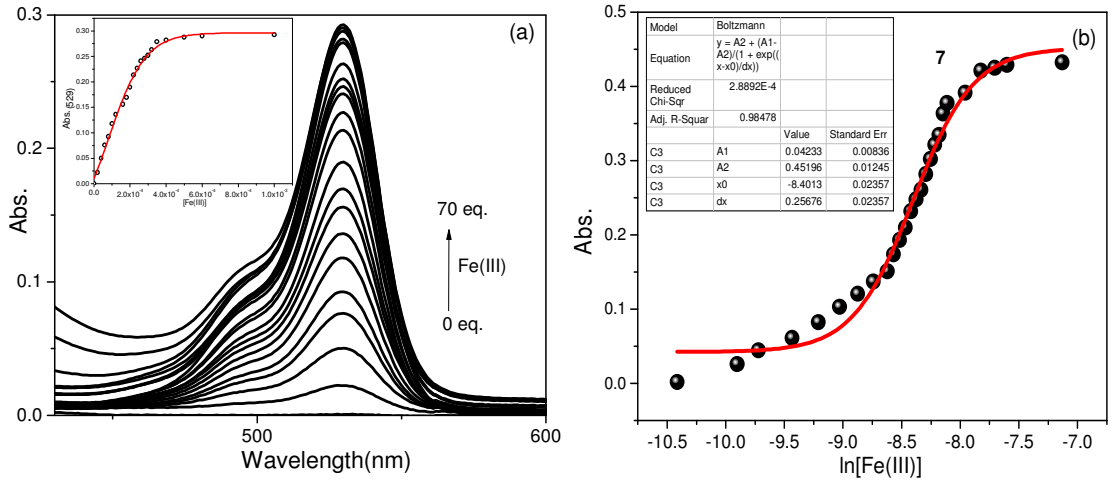

Fig. S61: (a) Absorption spectra of **7** with added Fe(III) ions in EtOH-H_2O (0.01M HEPES, 9:1 v/v), (b) non-linear fit to the plot of its corresponding intensities versus concentration (ln[Fe(III)]) for determination of Ka. [**7**] = 10 μM (abs.).

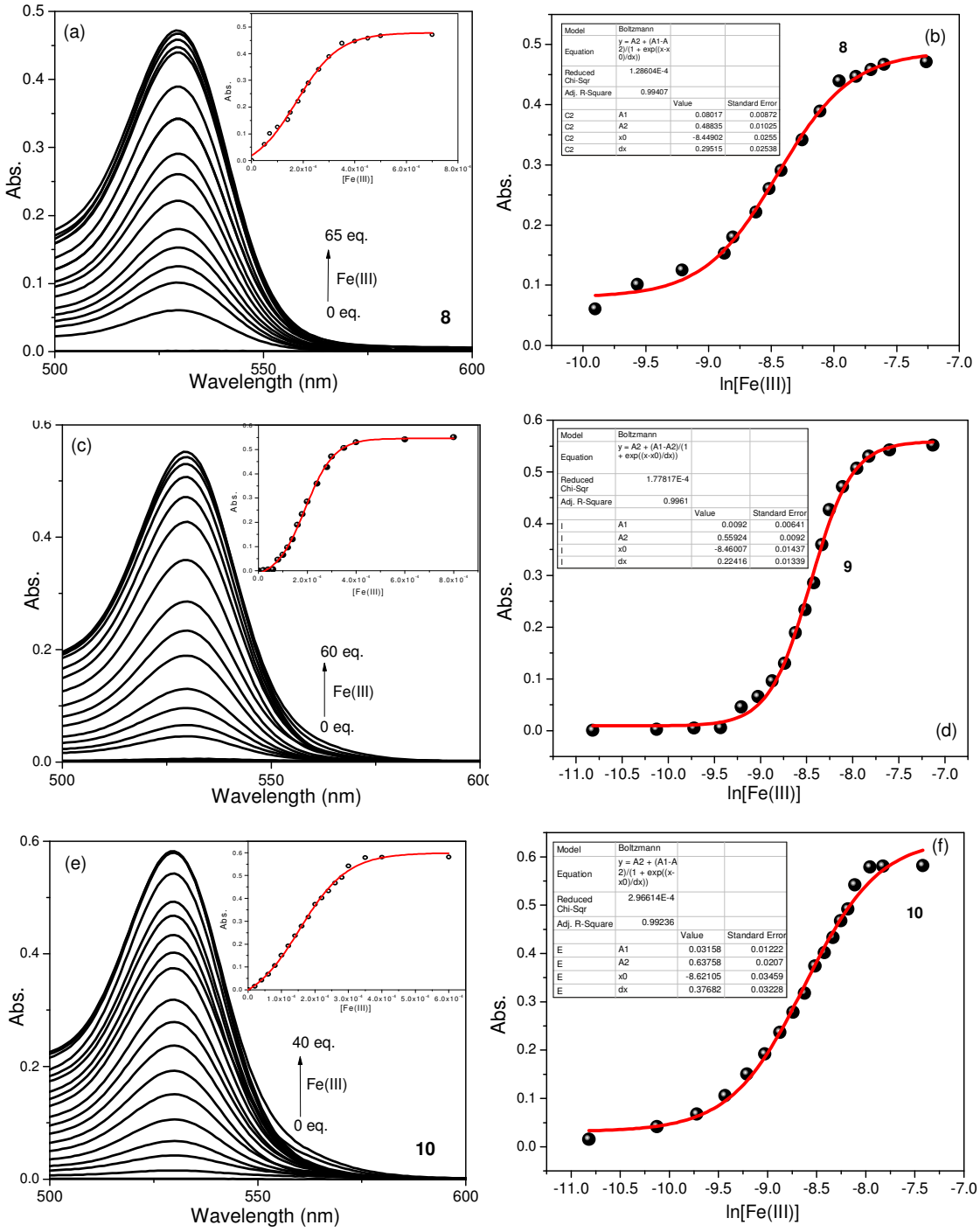

Fig. S62: (a) Absorption spectra (a, c and e) of **8, 9** and **10** on gradual addition of Fe(III) ions in EtOH-H_2O (0.01M HEPES, 9:1 v/v) medium, (b, d, f) Plot of their corresponding intensity versus concentration (ln[Fe(III)] and subsequent non-linear regressions for determination of corresponding Ka. [**8, 9, 10**] = 10 μM (abs.).

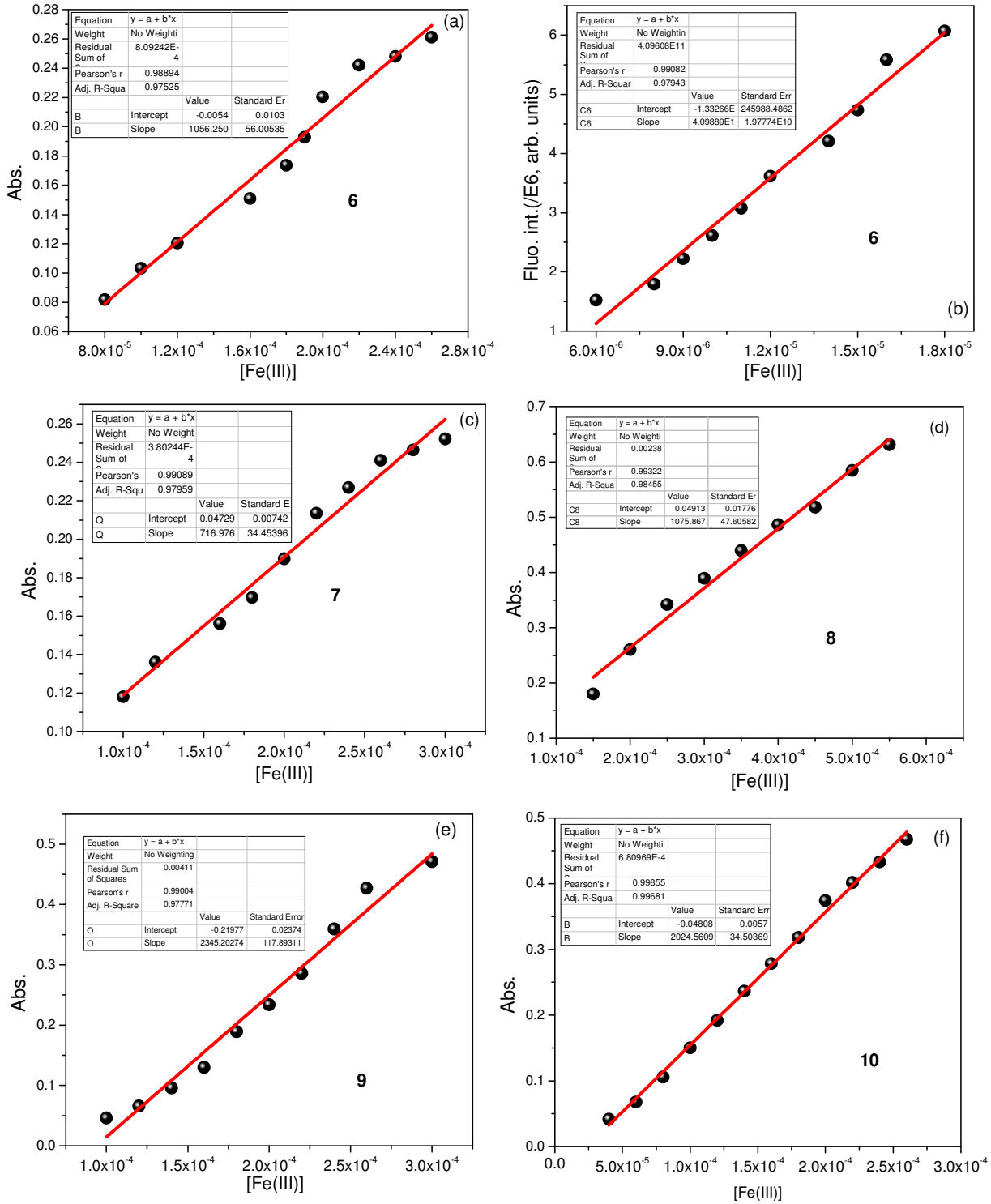

Fig. S63. Linear regression to the plot of absorbance of **6**-**10** (a, c, d, e, and f, respectively) and fluorescence intensities of **6** (b) on gradual addition of Fe(III) ion in a linear range for the determination of sensitivity of detection (S/N = 5).

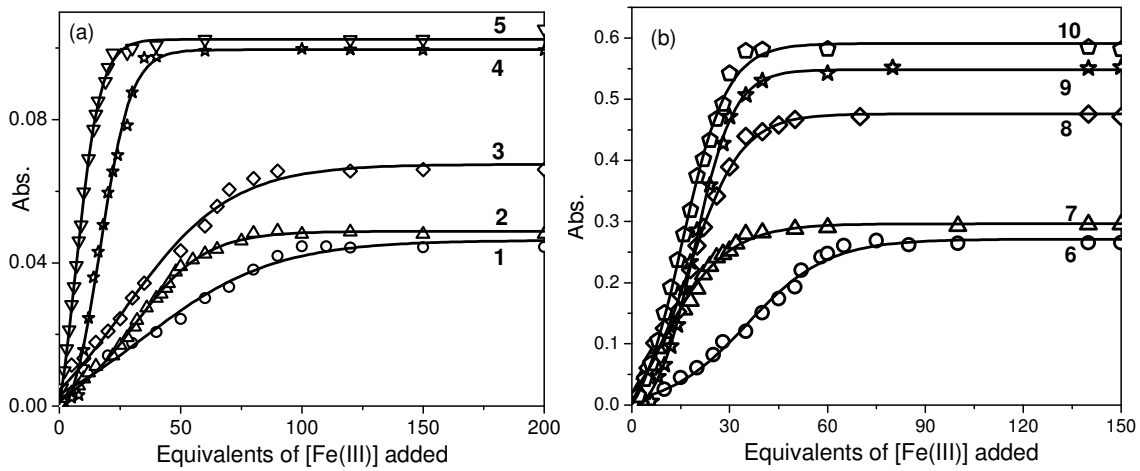

Fig. S64: Plot of absorbance of (a) **1**-**5** and (b) **6**-**10** on gradual addition of Fe(III) ions in EtOH-H_2O (0.01M HEPBS, 9:1 v/v), [probes] = 10 μM.

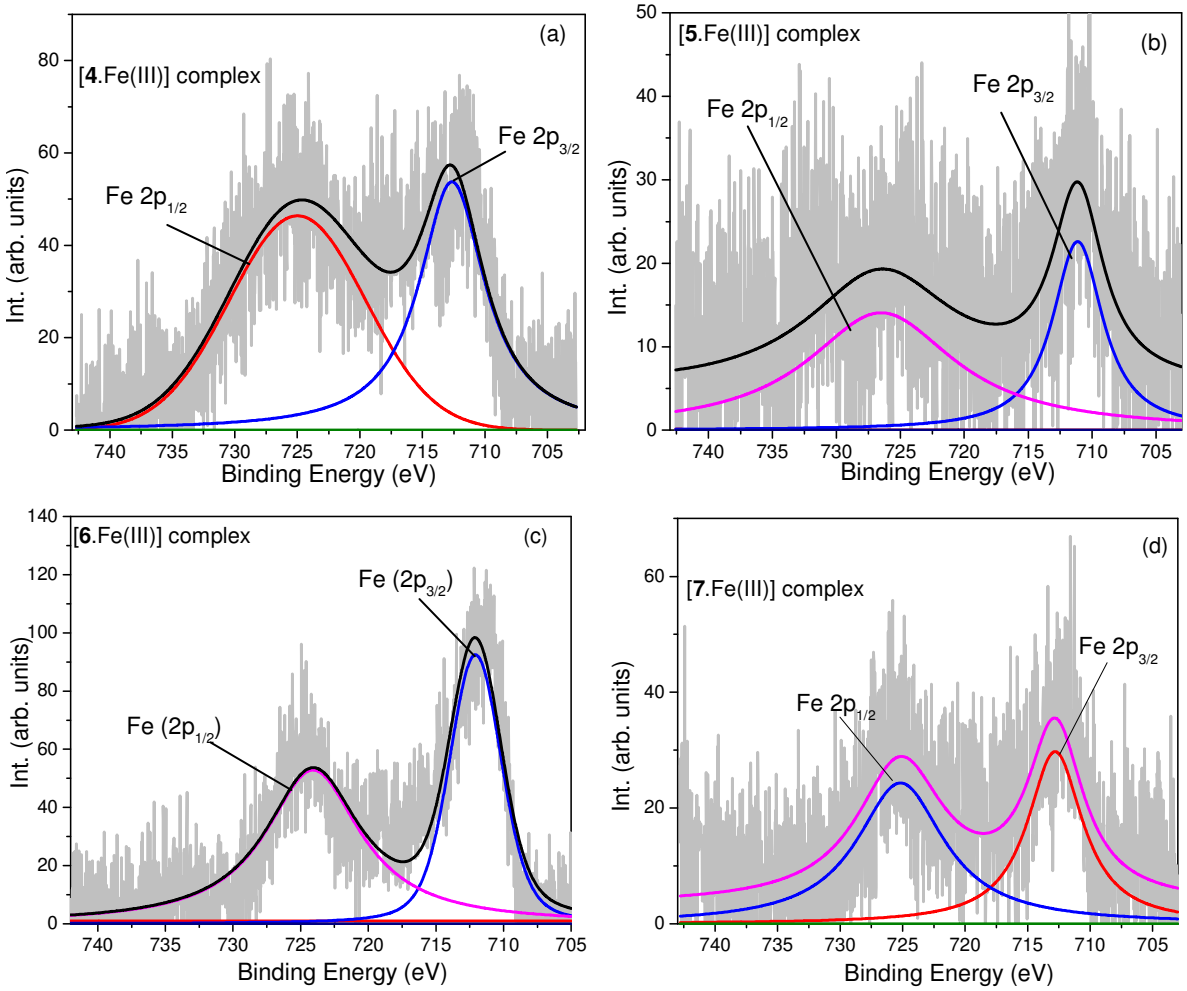

Fig. S65: Narrow-scan XPS spectral profile and corresponding component distribution fitting of Fe 2p region of Fe(III) complexes of **4** (a), **5** (b), **6** (c) and **7** (d).

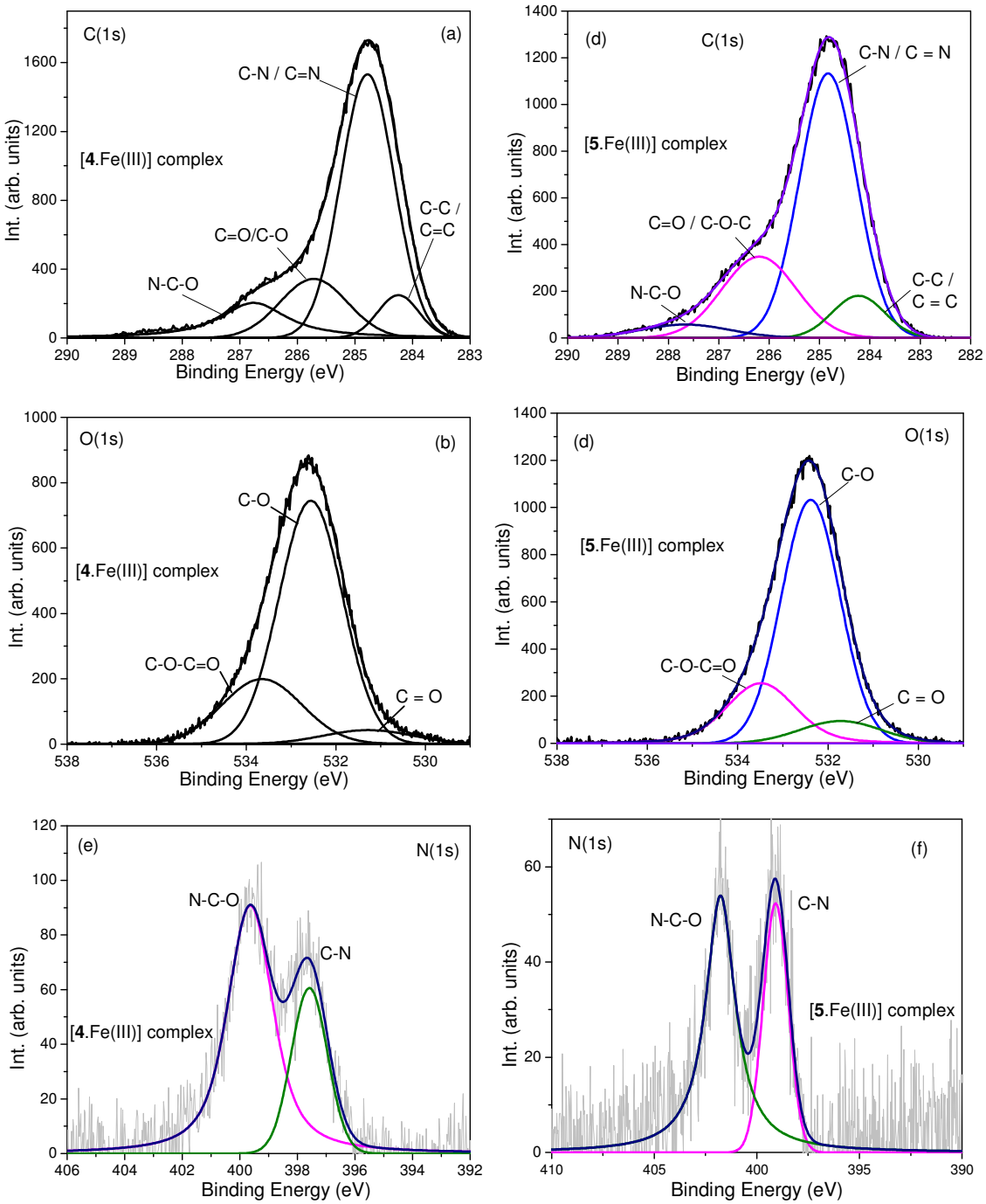

Fig. S66: Narrow-scan XPS spectral profile and corresponding component fitting of (a, d) C1s, (b, e) O1s and (c, f) N1s region in the Fe(III)-complexes of **4** (a, b, c) and **5** (d, e, f).

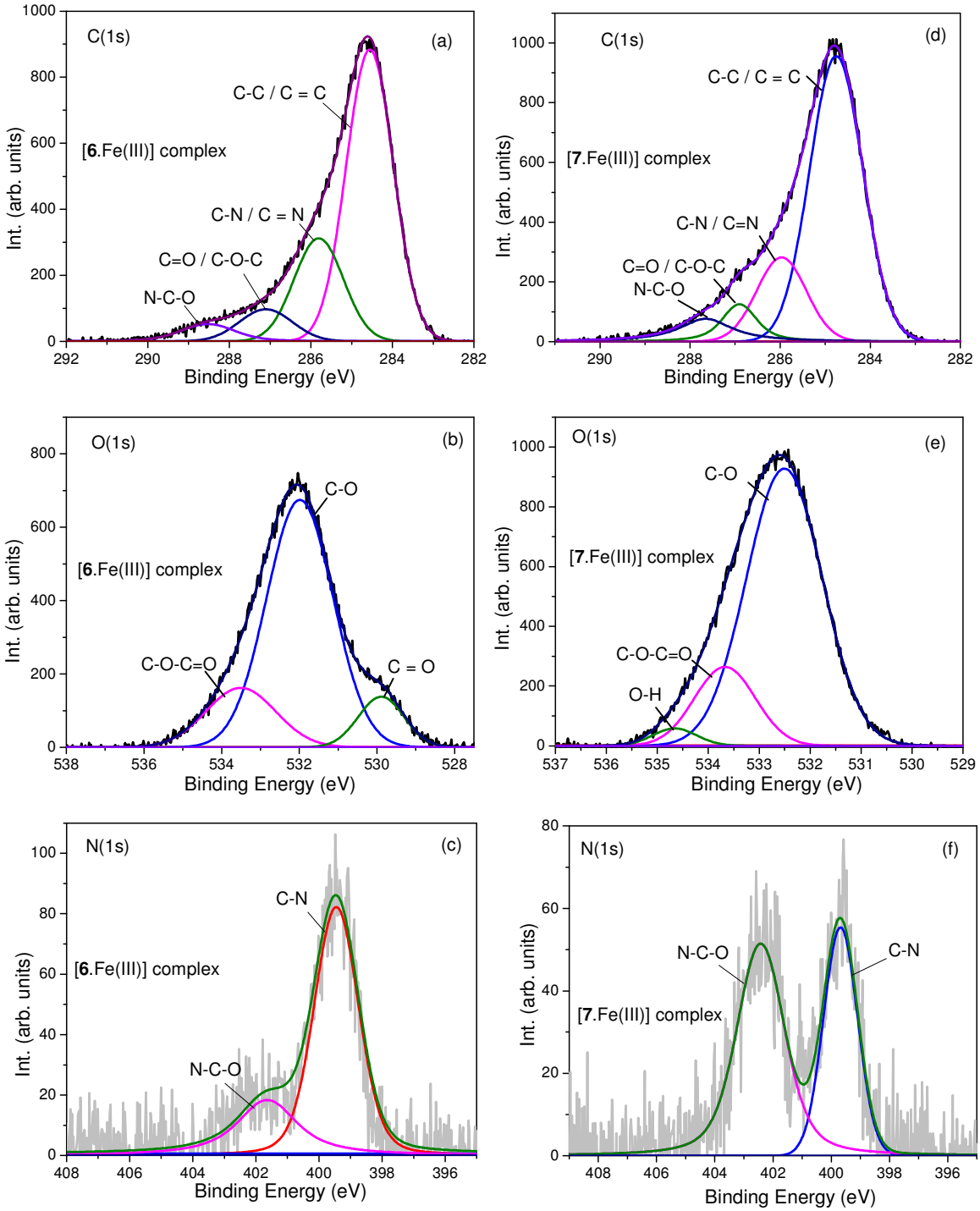

Fig. S67: Narrow-scan XPS spectral profile and corresponding component fitting of (a, d) C (1s), (b, e) O (1s) and (c, f) N (1s) region in the Fe(III) complexes of **6** (a, b, c) and **7** (d, e, f).

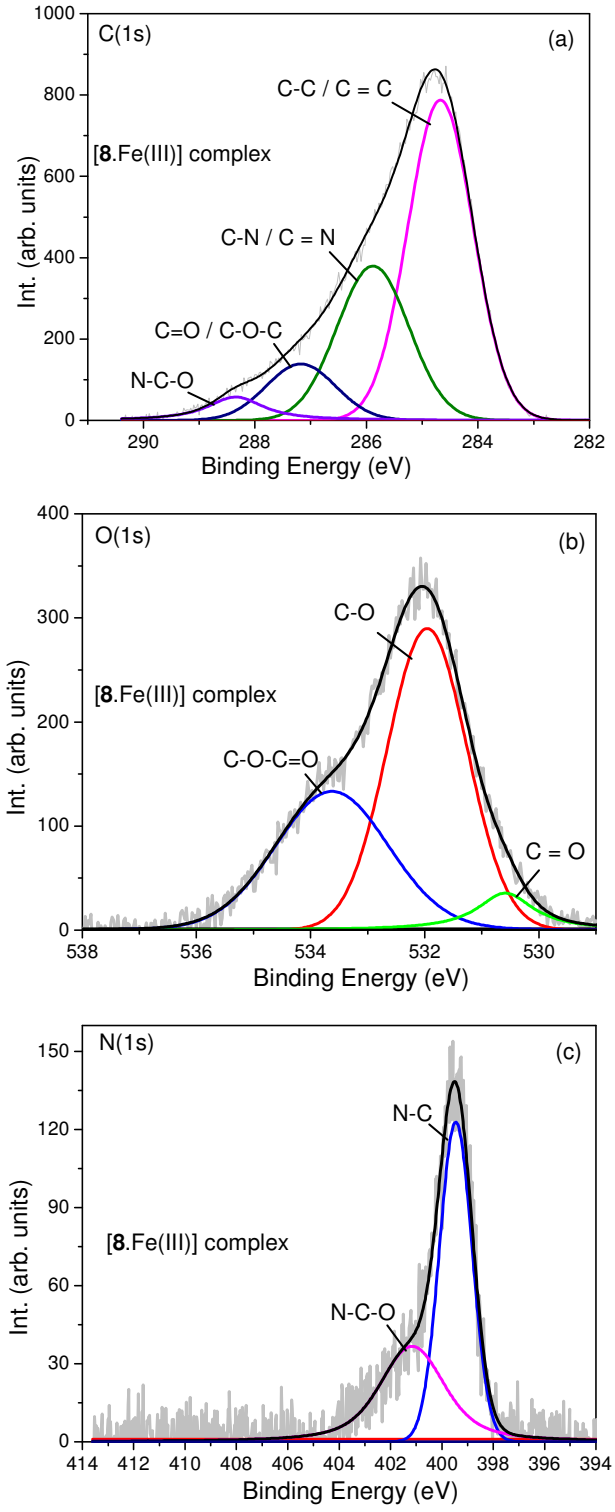

Fig. S68: Narrow-scan XPS spectral profile and corresponding component fitting of (a) C (1s), (b) O (1s) and (c) N (1s) region in the **8**-Fe(III) complex.

.

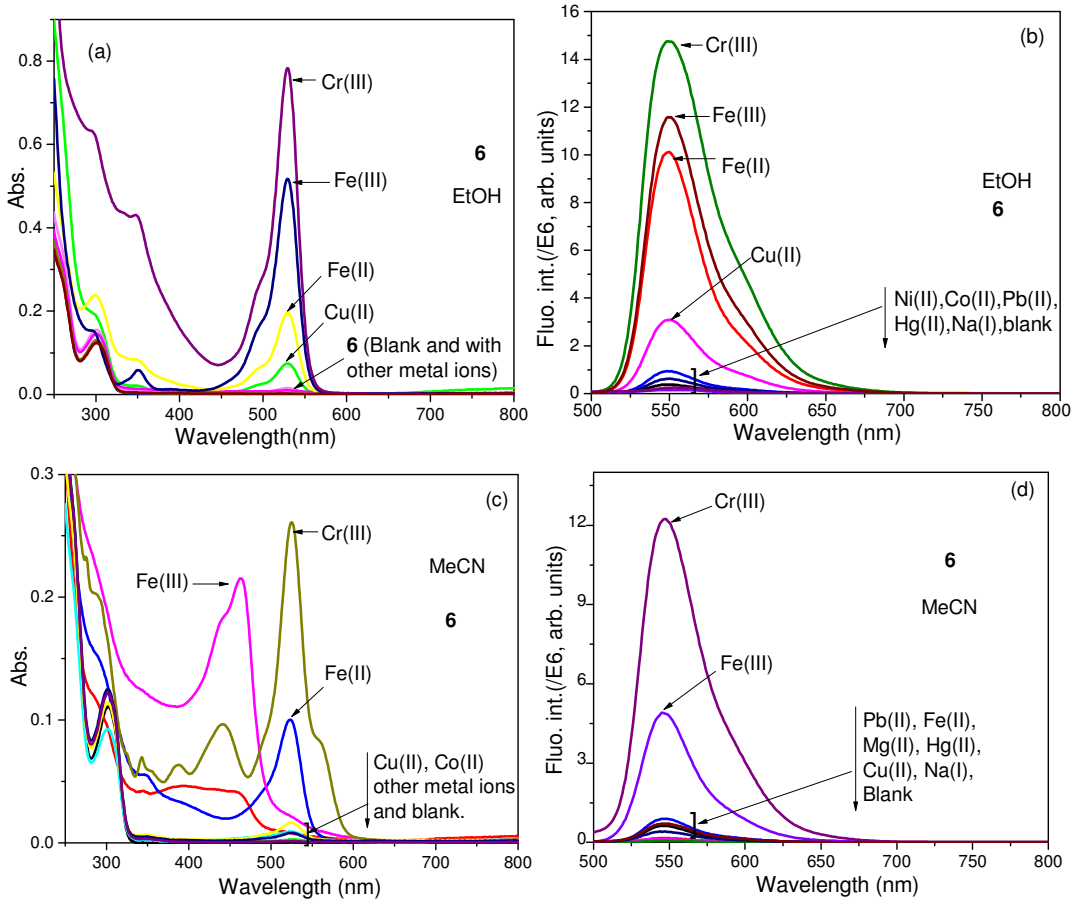

Fig. S69: Absorption (a, c) and fluorescence (b, d) spectral responses of **6** in presence of various metal ions in different solvents; in EtOH (a, b) and MeCN (c, d). *Conditions*: Abs.: [**6**] = 10 μM, Fluo.: [**6**] = 1 μM, [M(I/II/III] = 5 μM, em. and ex. band pass = 5 nm, λ_{ex} = 500 nm, RT. The probe **6** is responsive to multiple metal ions in pure organic solvents.

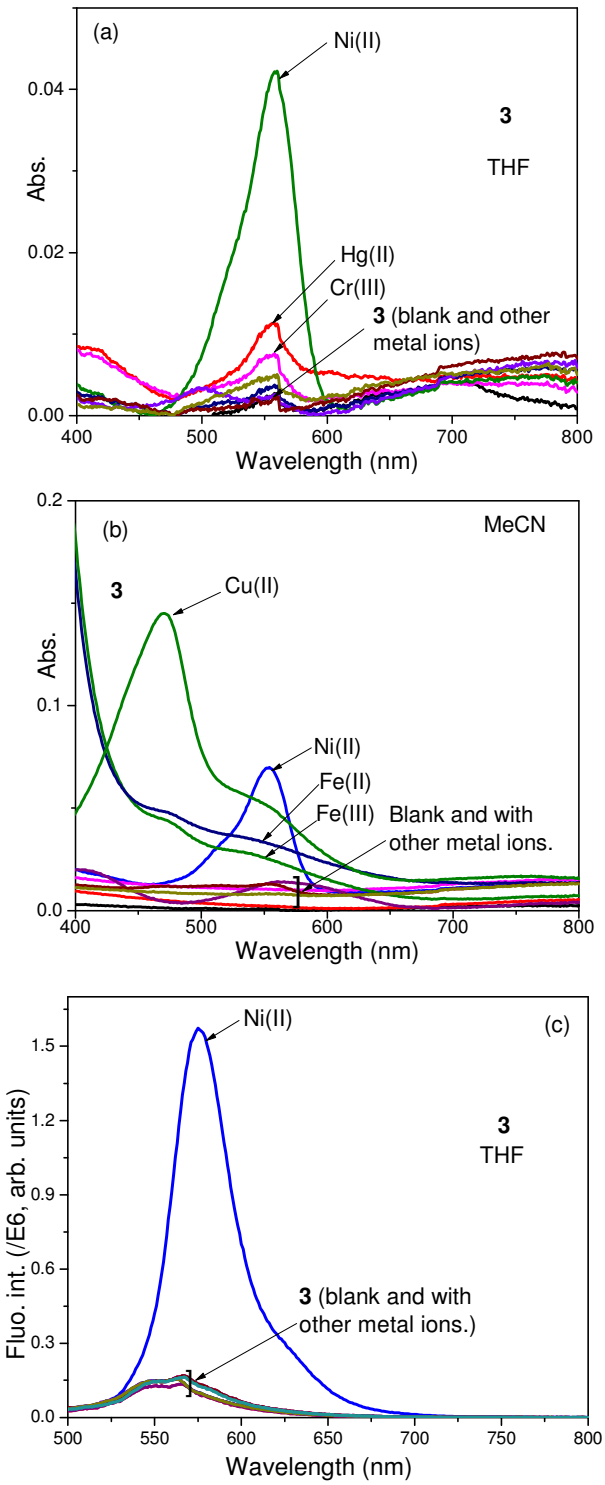

Fig. S70: Absorption spectra of **3** in (a) THF, (b) MeCN and Fluorescence (c) spectral responses of **3** in THF in presence of various metal ions. Conditions: Fluo.: [**3**]=1 μM, [M(I/II/III] = 5 μM, em. and ex. band pass = 5 nm, λ_{ex} = 500 nm, RT; This probe is responsive to multiple metal to ions in pure organic solvents.

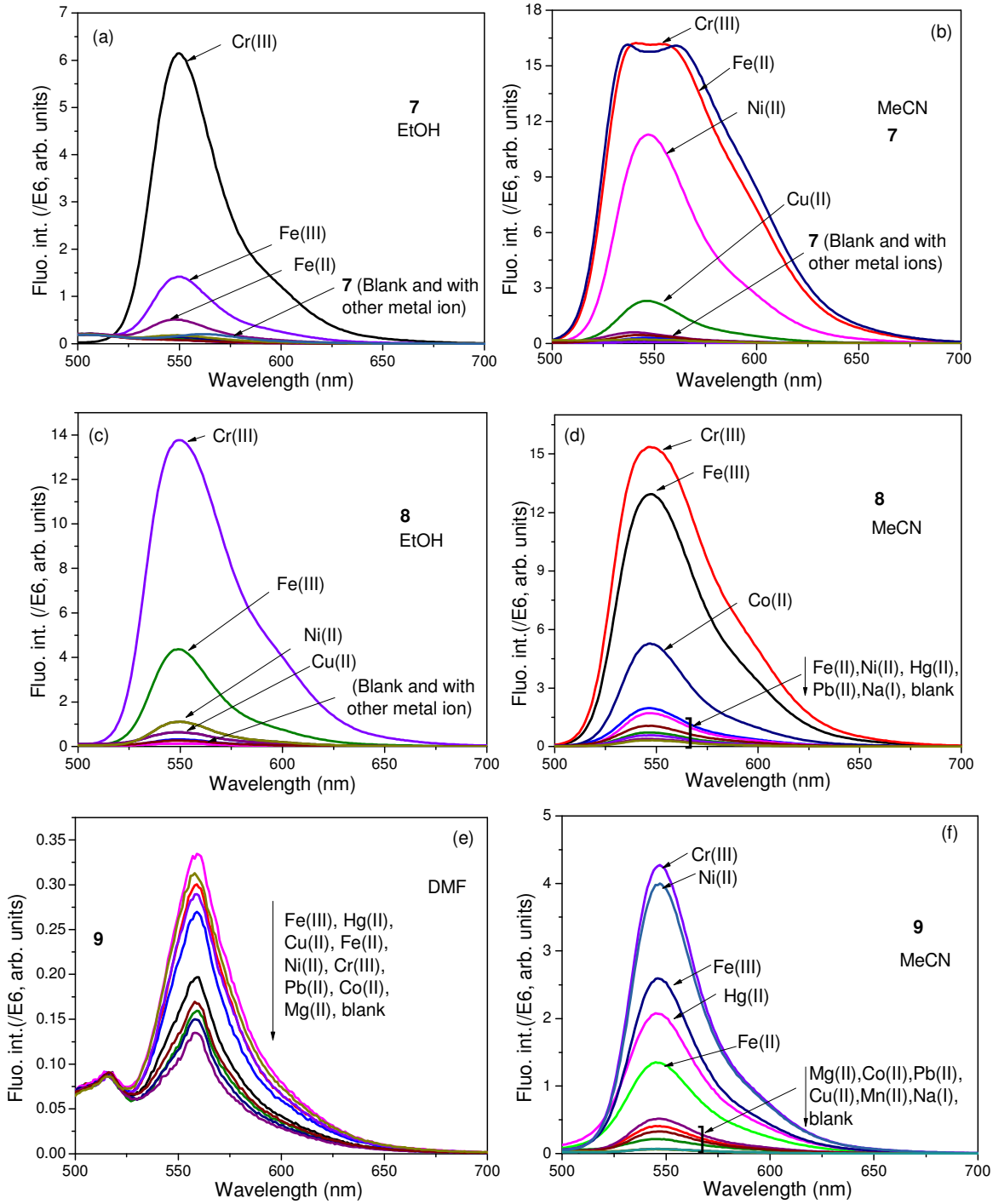

Fig. S71: Fluorescence spectra of **7** in (a) EtOH, (b) MeCN, that of **8** in (c) EtOH, (d) MeCN, and that of **9** in (e) DMF, (b) MeCN in presence of various metal ions. Conditions: Fluo.: [probes]=1 μM, [M(I/II/III] = 5 μM, em. and ex. band pass = 5 nm, λ_{ex} = 500 nm, RT; These probes are responsive multiple metal ions in pure organic solvents(THF, EtOH, DMF, MeCN).

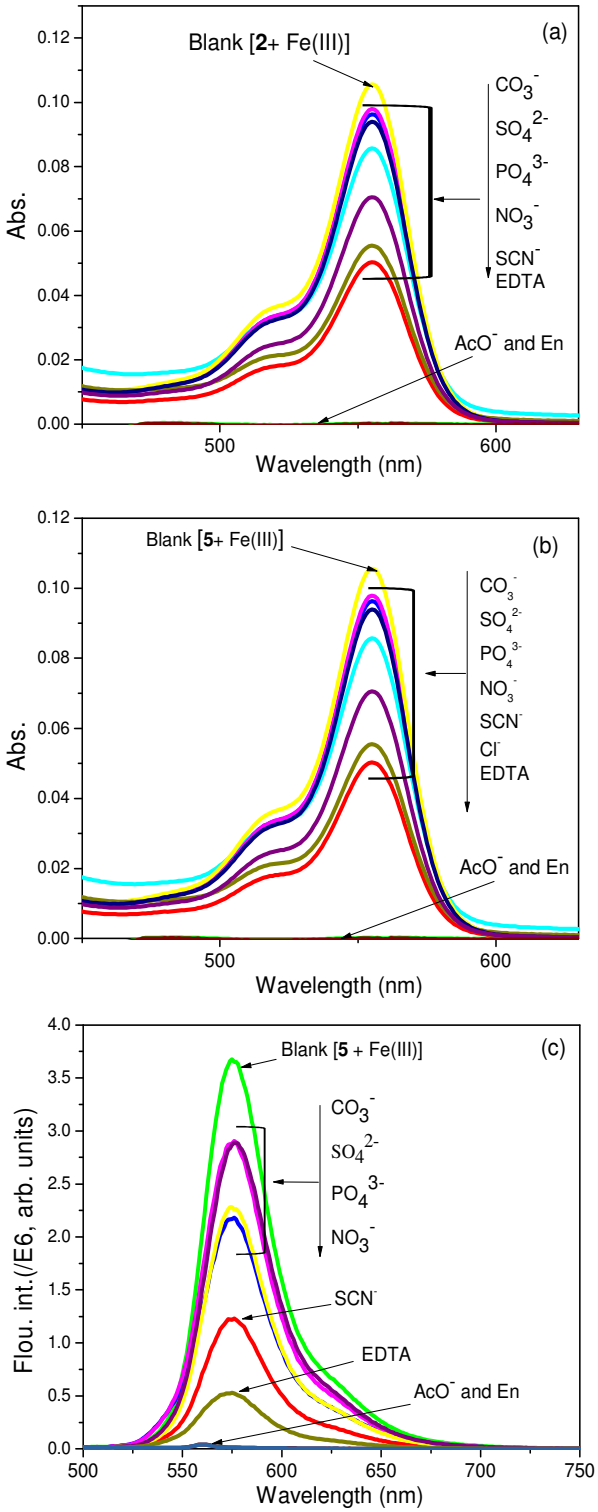

Fig. S72: Absorption spectral responses of Fe(III)-complexes of **2** and **5** in presence of various counter anions and chelating agents in EtOH-H_2O (0.01M HEPES, 9:1 v/v) showing reversibility in signalling of Fe(III) induced absorption (a, b) and fluorescence (c) enhancements.

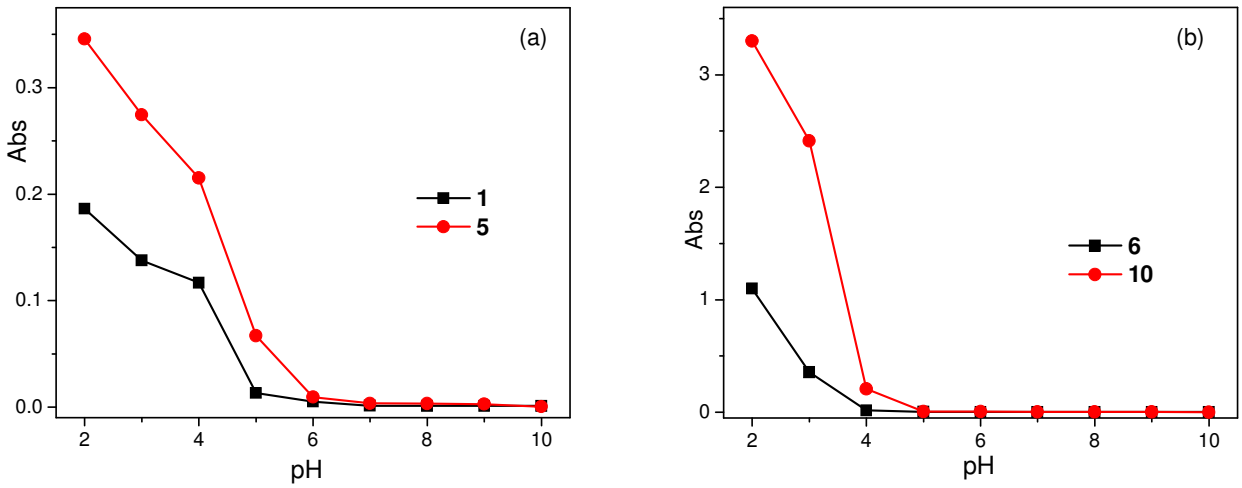

Fig. S73: Absorption spectral responses of (a) **1** and **5**, (b) **6** and **10** in EtOH-H_2O (9:1 v/v) under different pH conditions. [probes] = 100 μM.

Fig. S74: Photograph of the solutions of **1** (left) and **6** (right) at varying pH (2-10) values.

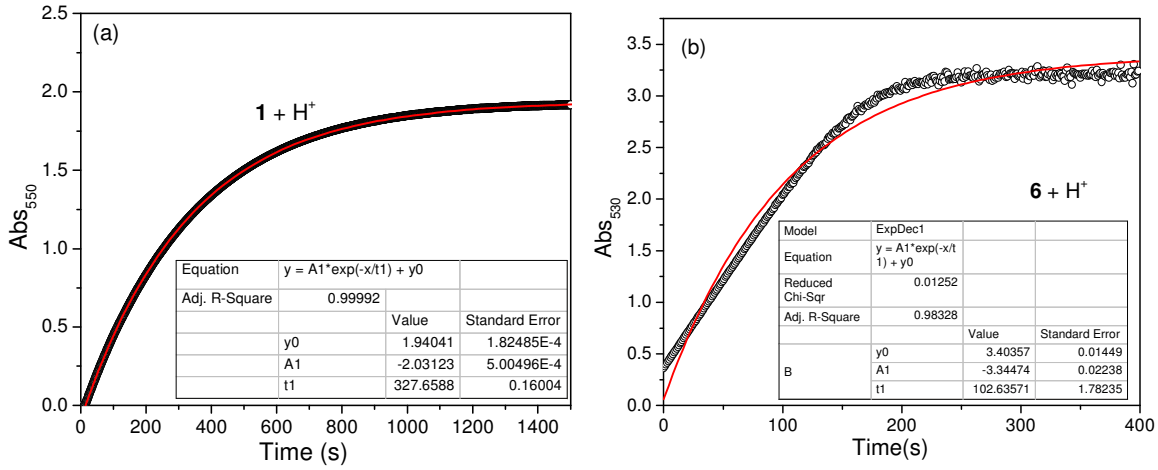

Fig. S75: Absorption spectral responses of (a) **1** and (b) **6** in presence of protons (perchloric acid) for determination of rate of proton-induced spiro-ring opening. [**1**] = [**6**] = 100 μM, in EtOH-H_2O (9:1 v/v, 0.01 HEPES).

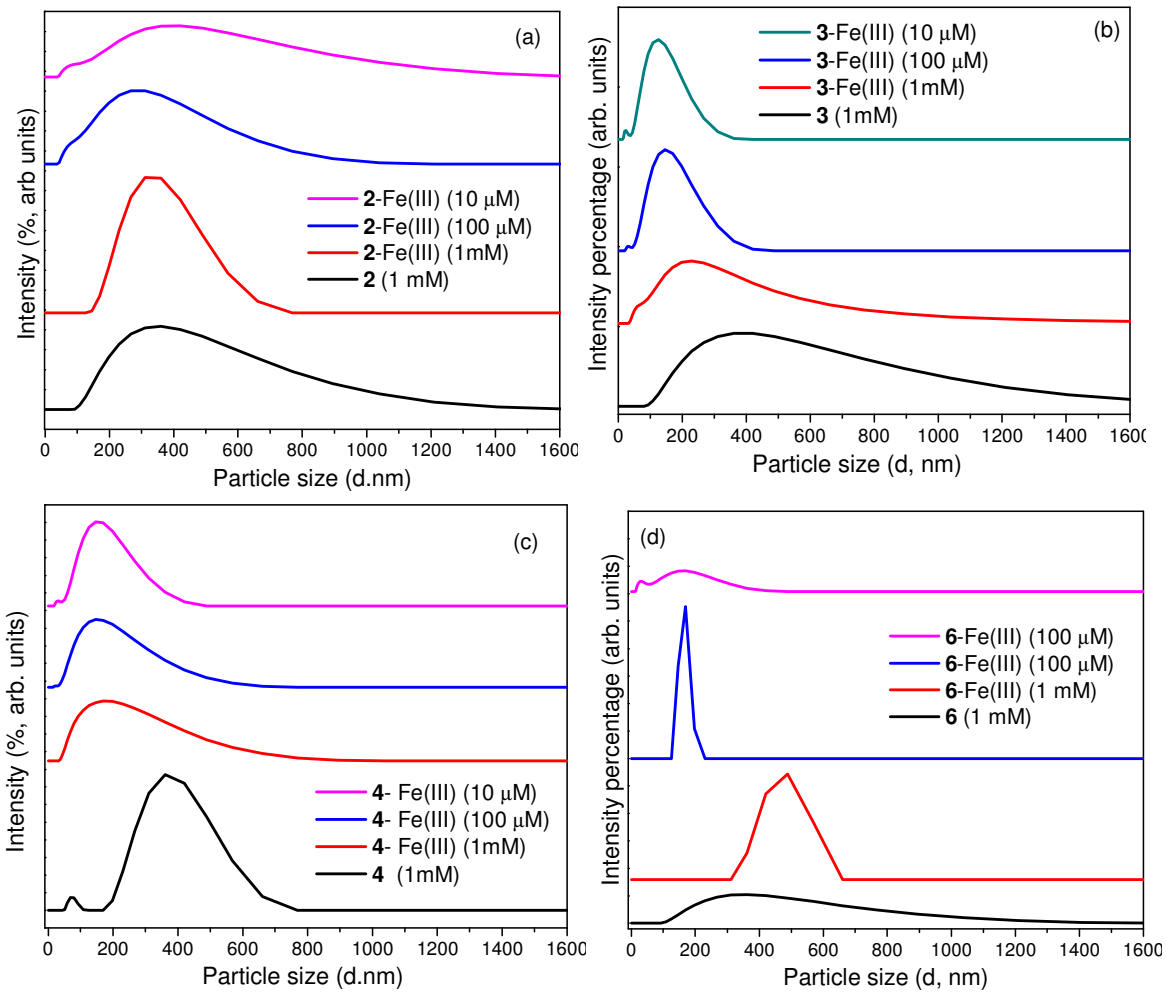

Fig. S76: Particle size of (a) **2**, (b) **3,** (c) **4** and (d) **6** and isolated solids of their Fe(III) complexes estimated through DLS measurements at different concentrations in EtOH-H_2O (0.01M HEPES, 9:1 v/v) medium. Similar spectral data of DLS measurements were obtained for other probes and their Fe(III) complexes towards comprehension of confirmation of the aggregate formation.

Table ST3: Particle size with poly-dispersive index (PDI) of the probes (**1**-**10**) and isolated solids of their Fe(III) complexes estimated through DLS measurements at different concentrations in EtOH-H_2O (0.01M HEPES, 9:1 v/v) medium.

Entry	Particle size of the aggregate (PDI)			
	1 μM	10 μM	100 μM	1mM
1	-	-	-	229 (0.823)
1-Fe(III)	-	-	-	535 (0.629)
2	-	-	-	333 (0.825)
2-Fe(III)	-	161 (0.669)	268 (0.359)	351 (0.458)
3	-	-	-	353 (0.699)
3-Fe(III)	-	122 (0.2605)	148 (0.248)	233 (0.441)
4	-	-	-	358 (0.501)
4-Fe(III)	-	148 (0.253)	188 (0.263)	180 (0.521)
5	-	-	-	145 (0.332)
5-Fe(III)	-	145 (0.610)	247 (0.244)	143 (0.318)
6	-	-	-	360 (0.556)
6-Fe(III)	-	152 (0.307)	172 (0.859)	490 (0.736)
7	-	-	-	361 (0.564)
7-Fe(III)	-	61 (0.856)	130 (0.568)	485 (0.825)
8	-	-	-	132 (0.825)
8-Fe(III)	-	138 (0.521)	111 (0.356)	248 (0.935)
9	-	-	-	420 (0.008)
9-Fe(III)	-	66 (0.591)	143 (0.666)	267 (0.957)
10	-	-	-	525 (0.309)
10-Fe(III)	-	59 (0.400)	169 (0.625)	424 (0.622)

“ -" could not be defined / high PDI

Following inferences from the experimental structural and electronic evidences for Fe(III) coordination to Rhodamine B based probes (**1**-**5**), the mechanism for Fe(III) coordination in the Rhodamine B based probes that resulted in photophysical signalling through complexation mediated spiro-ring opening is shown in the scheme (Scheme S1). The Rhodamine 6G based probes (**6**-**10**) too follow similar Fe(III) induced ring-opening mechanism.

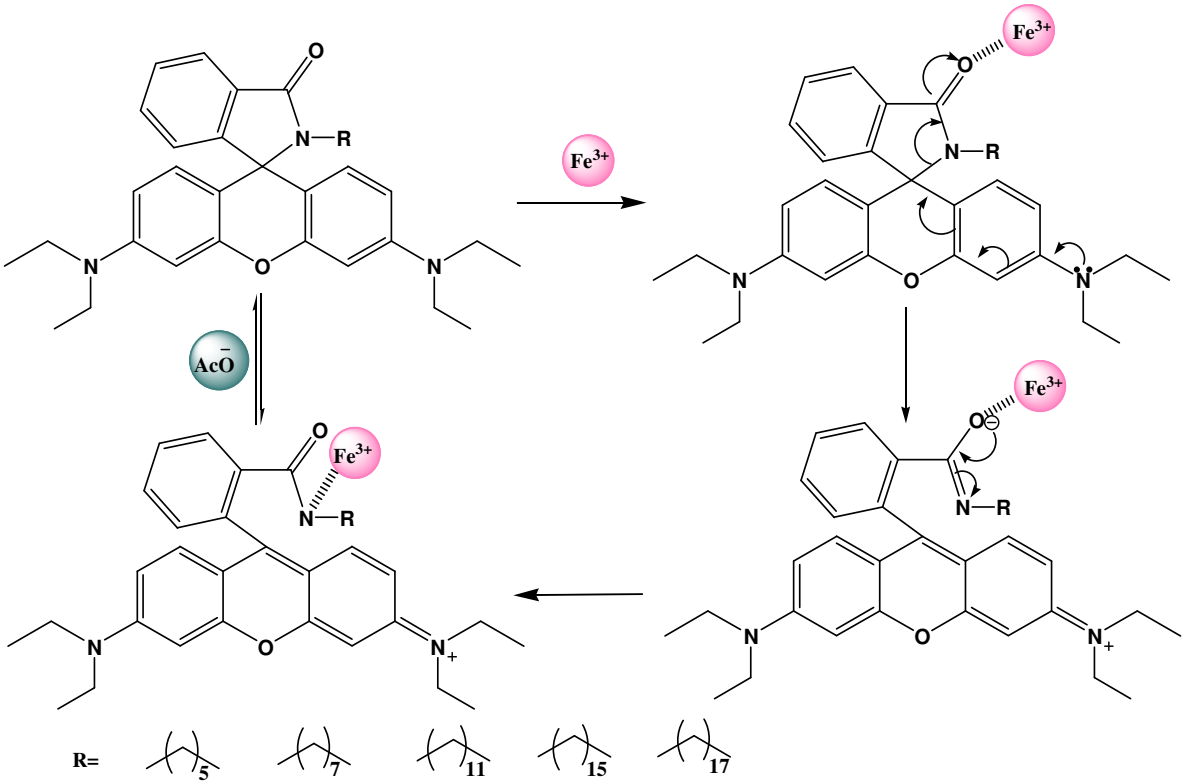

Scheme S1: Mechanistic pathway of Fe(III) complexation induced spiro-ring opening in Rhodamine B based probes leading to associated photophysical signalling pattern.